Intra-strain elicitation and suppression of plant immunity by *Ralstonia solanacearum* type-III effectors in *Nicotiana benthamiana*

Yuying Sang[1,#], Wenjia Yu[1,2,#], Haiyan Zhuang[1], Yali Wei[1,2], Lida Derevnina[3], Jiamin Luo[1,2] and Alberto P. Macho[1] *.

[1]Shanghai Center for Plant Stress Biology, CAS Center for Excellence in Molecular Plant Sciences; Shanghai Institutes of Biological Sciences, Chinese Academy of Sciences, Shanghai 201602, China.

[2]University of Chinese Academy of Sciences, Beijing, China.

[3]The Sainsbury Laboratory, University of East Anglia, Norwich Research Park, Norwich, NR4 7UH, United Kingdom.

[#] These authors contributed equally to this work.

* Corresponding author: Alberto P. Macho, alberto.macho@sibs.ac.cn

Keywords: cell death; ETI; SGT1; effector; immunity; virulence; Ralstonia; salicylic acid; jasmonic acid; ICS1; PAL

Abstract

Effector proteins delivered inside plant cells are powerful weapons for bacterial pathogens, but this exposes the pathogen to potential recognition by the plant immune system. Therefore, effector acquisition must be balanced for a successful infection. *Ralstonia solanacearum* is an aggressive pathogen with a large repertoire of secreted effectors. One of these effectors, RipE1, is conserved in most *R. solanacearum* strains sequenced to date. In this work, we found that RipE1 triggers immunity in *N. benthamiana*, which requires the immune regulator SGT1, but not EDS1 or NRCs. Interestingly, RipE1-triggered immunity induces the accumulation of salicylic acid (SA) and the overexpression of several genes encoding phenylalanine-ammonia lyases (PALs), suggesting that the unconventional PAL-mediated pathway is responsible for the observed SA biosynthesis. Surprisingly, RipE1 recognition also induces the expression of jasmonic acid (JA)-responsive genes and JA biosynthesis, suggesting that both SA and JA may act cooperatively in response to RipE1. Finally, we found that RipE1 expression leads to the accumulation of glutathione in plant cells, which precedes the activation of immune responses. *R. solanacearum* encodes another effector, RipAY, which is known to inhibit immune responses by degrading cellular glutathione. Accordingly, we show that RipAY inhibits RipE1-triggered immune responses. This work shows a strategy employed by *R. solanacearum* to counteract the perception of its effector proteins by the plant immune system.

Introduction

Ralstonia solanacearum is considered one of the most destructive plant pathogens, and is able to cause disease in more than 250 plant species (Jiang et al., 2017; Mansfield et al., 2012). As a soil-borne bacterial pathogen, *R. solanacearum* enters plants through the roots, reaches the vascular system, and spreads through xylem vessels, colonizing the plant systemically (Mansfield et al., 2012). This is followed by massive bacterial replication and the disruption of the plant vascular system, leading to eventual plant wilting (Digonnet et al., 2012; Turner et al., 2009).

Most bacterial pathogens deliver proteins inside plant cells via a type-III secretion system (T3SS); such proteins are thus called type-III effectors (T3Es) (Galan et al, 2014). T3Es have been reported to mediate the suppression of basal defenses and the manipulation of plant physiological functions to support bacterial proliferation (Macho et al, 2015; Macho, 2016). Resistant plants have evolved intracellular receptors defined by the presence of nucleotide-binding sites (NBS) and leucine-rich repeat domains (LRRs), thus termed NLRs (Cui et al, 2015). Specific NLRs can detect the activities of specific T3Es, leading to the activation of immune responses, which effectively prevent pathogen proliferation (Chiang & Coaker, 2015). The outcome of these responses is named effector-triggered immunity (ETI), and, in certain cases, may cause a hypersensitive response (HR) that involves the collapse of plant cells. Hormone-mediated signaling plays an essential role in plant immunity. Salicylic acid (SA) is considered the most important hormone in plant immunity against biotrophic pathogens (Vlot *et al.*, 2009; Burger & Chory, 2019); Jasmonic acid (JA), on the other hand, is considered the main mediator of immune responses against necrotrophic pathogens (Burger & Chory, 2019). In most cases, both hormones are considered as antagonistic, balancing the effects of each other (Burger & Chory, 2019).

In an evolutionary response to ETI, successful pathogens have acquired T3E activities to suppress this phenomenon (Jones & Dangl, 2006), although reports characterizing

T3E suppression of ETI remain scarce, particularly among T3Es within the same strain. While the development of additional T3E activities is a powerful virulence strategy, it also exposes the pathogen to further events of effector recognition. Therefore, the benefits and penalties of T3E secretion need to be finely and dynamically balanced in specific hosts, to ensure the appropriate manipulation of plant functions while evading or suppressing ETI. This balance may be particularly important for *R. solanacearum*, which secretes a larger number of T3Es in comparison to other bacterial plant pathogens (e.g. the reference GMI1000 strain is able to secrete more than 70 T3Es) (Peeters et al, 2013).

Plants have evolved to recognize immune elicitors from *R. solanacearum* (Wei et al, 2018; Jayaraman et al., 2016). In terms of mechanism of T3E recognition, the most studied case in *R. solanacearum* is RipP2 (also known as PopP2), which is perceived in Arabidopsis by the RRS1-RPS4 NLR pair (Gassmann et al, 1999; Deslandes et al, 2002; Tasset et al, 2010; Williams et al, 2014; Le Roux et al, 2015; Sarris et al, 2015). Additionally, several *R. solanacearum* T3Es were shown to induce cell death in different plant species (Peeters et al, 2013; Clarke et al, 2015), although, in most cases, it is unclear whether these are due to toxic effects caused by effector overexpression or a host immune response. Some *R. solanacearum* T3Es have also been shown to cause a restriction of host range; such is the case for RipAA and RipP1 (also known as AvrA and PopP1, respectively), which are perceived and restrict host range in *Nicotiana* species (Poueymiro et al, 2009). RipP1 also triggers resistance in petunia (Lavie et al, 2002). Similarly, RipB-triggered immunity has been reported as the major cause for avirulence of *R. solanacearum* RS1000 in *Nicotiana* species (Nakano & Mukaihara, 2019), RipAX2 (also known as Rip36) have been shown to induce resistance in eggplant and its wild relative *Solanum torvum* (Nahar et al, 2014; Morel et al, 2018), and several T3Es from the AWR family (also known as RipA) restrict bacterial growth in Arabidopsis (Sole et al, 2012). Although the utilization of these recognition systems to generate disease-resistant crops is tantalizing, it is imperative to understand the mechanisms underlying the activation of plant immunity and their

potential suppression by other T3Es within *R. solanacearum*.

The *ripE1* gene encodes a protein secreted by the type-III secretion system in the *R. solanacearum* GMI1000 strain (phylotype I) (Mukaihara et al, 2010), and is conserved across *R. solanacearum* strains from different phylotypes (Peeters et al, 2013). Based on sequence analysis, RipE1 is homologous to other T3Es in *Pseudomonas syringae* (HopX) and *Xanthomonas spp* (XopE) (Figure S1; Peeters et al, 2013), belonging to the HopX/AvrPphB T3E family (Nimchuk et al, 2007). This family is characterized by the presence of a putative catalytic triad consisting of specific cysteine, histidine, and aspartic acid residues, which are conserved in RipE1 (Nimchuk et al, 2007; Figure S1), and is similar to several enzyme families from the transglutaminase protein superfamily, such as peptide N-glycanases, phytochelatin synthases, and cysteine proteases (Makarova et al, 1999). AvrPphB, from *P. syringae* pv. *phaseolicola*, the original member of the HopX/AvrPphB family, was identified based on its ability to activate immunity in certain bean cultivars (Mansfield et al, 1994). Divergent members from this family in other strains also trigger immunity, and this requires the putative catalytic cysteine (Nimchuk et al, 2007). Previous sequence analysis of T3Es from the HopX family also identified a conserved domain (domain A) required for HopX induction of immunity in bean and Arabidopsis, which as hypothesized to represent a host-target interaction domain or a novel nucleotide/cofactor binding domain (Nimchuk et al, 2007).

In this work, we studied the impact of RipE1 in plant cells, and found that RipE1 is recognized by the plant immune system in both *N. benthamiana* and Arabidopsis, leading to the activation of immune responses. We further investigate the immune components and signaling pathways associated to this effector recognition. Finally, we found that another effector in *R. solanacearum* GMI1000 is able to inhibit RipE1-triggered immune responses in *N. benthamiana*, explaining the fact that RipE1 does not seem to be an avirulence determinant in this plant species.

Results

RipE1 triggers cell death upon transient expression in *Nicotiana benthamiana*

In order to understand the impact of RipE1 in plant cells, we first used an *Agrobacterium tumefaciens* (hereafter, Agrobacterium)-mediated expression system in *Nicotiana benthamiana* leaves to transiently express RipE1 that is fused to a carboxyl-terminal green fluorescent protein (GFP) tag (RipE1-GFP). Two days after Agrobacterium infiltration, we noticed the collapse of infiltrated tissues expressing RipE1-GFP, but not a GFP control (Figure 1a). This tissue collapse correlated with a release of ions from plant cells (Figure 1b), indicative of cell death. Mutation of the catalytic cysteine to an alanine residue has been shown to disrupt the catalytic activity of enzymes with a catalytic triad similar to that conserved in RipE1 (Gimenez-Ibanez et al, 2014; Figure 1c). To determine if the putative catalytic activity is required for RipE1 induction of cell death, we generated an equivalent mutant in RipE1 (C172A; Figure 1c). We also generated an independent mutant with a deletion on the eight amino acids that constitute the conserved domain A (Nimchuk et al, 2007; Figure 1c). These mutations did not affect the accumulation of RipE1 (Figure 1d), but abolished the induction of tissue collapse and the ion leakage caused by RipE1 expression (Figure 1d and 1e), indicating that RipE1 requires both the catalytic cysteine and the conserved domain A for the induction of cell death in plants.

Interestingly, RipE1 was also identified in a systematic screen performed in our laboratory to identify *R. solanacearum* T3Es that suppress immune responses triggered by bacterial elicitors. In this screen we found that RipE1 expression suppresses the burst of reactive oxygen species (ROS) and the activation of mitogen-activated protein kinases (MAPKs) triggered upon treatment with the bacterial flagellin epitope flg22, which acts as an immune elicitor (Figure S2). RipE1 requires both the catalytic cysteine and the conserved domain A for this activity (Figure S2). However, we considered the possibility that these responses are abolished by the

death of plant cells rather than an active immune suppression. Time-course experiments showed that the suppression of flg22-triggered ROS correlated with the appearance of cell death (Figure S2), making it difficult to uncouple these observations.

RipE1 activates salicylic acid-dependent immunity in *N. benthamiana*

The induction of cell death by pathogen effectors may reflect toxicity in plant cells or the activation of immune responses that lead to HR. Salicylic Acid (SA) plays a major role in the activation of immune responses after the perception of different types of invasion patterns (Vlot *et al.*, 2009). To determine whether RipE1 activates immune responses, we first measured the expression of the *N. benthamiana* ortholog of the Arabidopsis gene *PATHOGENESIS-RELATED-1* (*PR1*), which is a hallmark of SA-dependent immune responses (Vlot et al., 2009, Ward *et al.*, 1991). Expression of RipE1-GFP (but not the C172A catalytic mutant) significantly enhanced the accumulation of *NbPR1* transcripts (Figure 2a). The bacterial salicylate hydroxylase NahG converts SA to catechol and leads to the suppression of SA-dependent responses (Delaney et al., 1994). The expression of NahG-GFP in *N. benthamiana* slightly enhanced the accumulation of RipE1 fused to a carboxyl-terminal N-luciferase tag (Nluc) (Figure S3), consistent with the reported role of SA in hindering Agrobacterium-mediated transformation (Rosas-Diaz et al, 2016); despite this, NahG partially suppressed RipE1-triggered cell death, ion leakage, and *NbPR1* expression (Figure 2b, c and d). Altogether, these data suggest that RipE1 induces SA-dependent immune responses in plant cells, which cause the development of HR cell death.

RipE1 enhances the expression of *PAL* genes and the biosynthesis of salicylic acid and jasmonic acid

The expression of RipE1 led to a dramatic increase in SA accumulation in *N. benthamiana* (Figure 3a), consistent with the observed overexpression of *NbPR1*

(Figure 2a). This reinforces the idea that RipE1 is perceived by the plant immune system and this leads to the activation of SA biosynthesis and SA-dependent immune responses. In Arabidopsis, the chloroplastic pathway mediated by isochorismate synthethase 1 (ICS1) plays a predominant role in the pathogen-induced SA biosynthesis (Wildermuth et al, Nature, 2001; Garcion et al, Plant Physiology, 2008). However, gene expression analysis showed that the expression of the *N. benthamiana* ortholog of the Arabidopsis *ICS1*, *NbICS1*, was significantly reduced upon RipE1 expression (Figure 3b), despite the simultaneous high *NbPR1* transcript accumulation (Figure 2a). SA can also be synthesized from phenylalanine in a pathway mediated by phenylalanine ammonia lyases (PALs). In contrast with the expression of *NbICS1*, several genes encoding NbPALs were up-regulated upon expression of RipE1, but not the catalytic mutant version (Figure 3c-e), suggesting that this pathway may mediate the enhancement in SA biosynthesis upon perception of RipE1 activity. SA and Jasmonic Acid (JA) are considered antagonistic hormones in plant immune responses. Surprisingly, instead of a reduction of JA-associated gene expression, we found a slight increase in the accumulation of *NbLOX2* transcripts in early time points upon expression of catalytically active RipE1 (Figure 3f). In Arabidopsis, LOX2 contributes to the biosynthesis of JA (Bell et al, 1995). Accordingly, we detected an increase in JA contents upon RipE1 expression (Figure S4), indicating that RipE1 perception does not inhibit JA signalling, but rather leads to an enhancement on JA biosynthesis and associated gene expression.

RipE1-triggered immunity requires SGT1, but not EDS1 or NRC proteins

The suppressor of the G2 allele of *skp1* (SGT1) plays an essential role in ETI, and is required for the induction of disease resistance mediated by most NLRs (Azevedo *et al.*, 2002; Kadota *et al.*, 2010). Virus-induced gene silencing (VIGS) of *NbSGT1* abolished RipE1-triggered cell death, ion leakage, and *NbPR1* expression (Figure 4a-d), indicating that RipE1-triggered immunity requires SGT1. While most NLRs require SGT1 to function, a specific group of NLRs containing an N-terminal Toll-like

interleukin-1 receptor (TIR) domain also require EDS1 (Wiermer et al, 2005; Schultink et al, 2017). *N. benthamiana* plants carrying a stable knockout mutation in *EDS1* (Schultink et al, 2017) displayed clear RipE1-triggered cell death (Figure 4e), suggesting that RipE1-triggered immunity is not mediated by a TIR-NLR. Other NLRs contain a C-terminal coiled coil (CC) domain, and a specific subset of CC-NLRs require a network of helper NLRs termed NRC proteins (Wu et al, 2016). Interestingly, silencing of NRC proteins did not impact RipE1-triggered cell death (Figure S5), suggesting that RipE1-triggered immunity is not mediated by an NLR within the NRC network.

RipE1 activates immunity in Arabidopsis

Arabidopsis transgenic plants expressing RipE1-GFP from a *35S* inducible promoter died after germination (data not shown). Therefore, we generated Arabidopsis transgenic plants expressing RipE1-GFP and RipE1^{C172A}-GFP from an estradiol (EST)-inducible promoter. Five week-old plants expressing RipE1-GFP, but not RipE1^{C172A}-GFP, showed reduced growth in soil upon EST treatment for 14 days (Figure 5a). To determine whether RipE1-triggered growth reduction in Arabidopsis correlates with the activation of immunity, we first monitored the expression of defence-related genes. Similar to the result observed upon expression in *N. benthamiana*, expression of RipE1 in Arabidopsis triggered the overexpression of *AtPR1* (Figure 5b). However, in Arabidopsis, the enhanced *PR1* expression correlated with an overexpression of *AtICS1*, but not *AtPAL1*, upon RipE1 expression (Figure 5b). As observed in *N. benthamiana*, RipE1 expression led to the overexpression of the JA marker genes *AtVSP2* and *AtPDF1*.2 (REF; Figure 5b). This indicates that, as observed in *N. benthamiana*, RipE1 activates SA- and JA-dependent signalling in Arabidopsis. To determine whether the activation of defence-related genes leads to an efficient immune response in Arabidopsis, we inoculated RipE1-expressing plants by soil-drenching with *R. solanacearum*. As shown in the figure 5c, RipE1-expressing plants displayed weaker and delayed disease symptoms upon *R. solanacearum*

inoculation, reflecting an enhanced disease resistance upon *RipE1* expression.

RipE1-triggered immune responses are suppressed by RipAY

RipE1 expression activates immunity in Arabidopsis and *N. benthamiana*, although both plant species are susceptible hosts for *R. solanacearum* GMI1000 (or a derivative strain carrying mutations in *popP1* and *avrA*, in the case of *N. benthamiana*; Poueymiro et al, 2009), which carries RipE1. Therefore, we reasoned that other T3E(s) in GMI1000 may be able to suppress RipE1-triggered immunity in the context of infection. We recently identified a *R. solanacearum* T3E, RipAY, which is able to suppress SA-dependent immune responses through the degradation of glutathione (Sang et al, 2016; Mukaihara et al, 2016); however, the ability of RipAY to suppress immunity triggered by other *R. solanacearum* T3Es remained unknown. Interestingly, the expression of RipE1 in *N. benthamiana* leads to an increase in glutathione accumulation in plant tissues, which precedes the onset of immune responses (Figure 6a). Considering that both RipAY and RipE1 are present in GMI1000, we sought to determine if RipAY has the ability to suppress RipE1-triggered immunity. Indeed, expression of RipAY in *N. benthamiana* did not affect the accumulation of RipE1 (Figure S6), but abolished the tissue collapse and ion leakage caused by RipE1 expression (Figure 6b, c, and d). Moreover, RipAY was able to suppress the overexpression of *NbPR1* triggered by RipE1 (Figure 6e), indicating that RipAY suppresses RipE1-triggered immune responses. Interestingly, however, a RipAY point mutant unable to degrade glutathione (RipAY^{E216Q}; Sang et al, 2016) did not suppress RipE1-triggered responses (Figure 6b-e), suggesting that RipAY suppresses RipE1-triggered immunity through the degradation of cellular glutathione.

Discussion

Expression of T3Es in plant cells may either induce cell death because of cell toxicity or lead to the activation of an immunity-associated HR. Over-expression of RipE1 in *N. benthamiana* leads to cell death that: (*i*) is dependent on the immune regulator SGT1; (*ii*) activates SA accumulation and *PR1* expression; and (*iii*) is suppressed by the NahG and other *R. solanacearum* effectors, indicating that RipE1-mediated cell death is due to the activation of immunity in the host. Several T3Es within the HopX/AvrPphB family are predicted enzymes that are associated with activation of host immunity, although the association of the predicted catalytic activity with the activation of immunity seems to be differ among them. While the ability of AvrPphB and several other family members to trigger immunity requires the putative catalytic cysteine (Mansfield et al, 1994; Nimchuk et al, 2007), other members with the predicted catalytic activity, such as HopX from *P. syringae* pv *tabaci* or *P. syringae* pv *phaseolicola* race 6, do not trigger immunity in the same hosts (Stevens et al, 1998; Nimchuk et al, 2007). In the case of RipE1, the putative catalytic cysteine is required for the induction of immunity, which suggests that RipE1 is an active enzyme, and that this catalytic activity leads to perception by the host immune system. Moreover, the conserved domain A (Nimchuk et al, 2007) is also required for the activation of immunity by RipE1. In addition, we found that RipE1 is able to suppress elicitor-triggered immune responses in *N. benthamiana*. However, since this activity correlates with the induction of cell death, it is difficult to uncouple both observations, and further studies on the virulence activity of RipE1 will require the utilization of a host plant that is unable to recognize it.

The fact that RipE1 is recognized, and activate immune responses, in both *N. benthamiana* and Arabidopsis suggests at least two scenarios: it is possible that the NLR responsible for this recognition is conserved in both species; on the other hand, it is also possible that both species have independently develop NLRs that recognize RipE1. Although we did not identify the NLR involved, we determined that, at least in *N.*

benthamiana, RipE1 recognition does not rely on EDS1 or the NRC network, pointing to a CC- NRC-independent NLR. Interestingly, although RipE1 perception leads to the accumulation of SA in both plant species, the associated gene expression patterns seem to differ. The ICS pathway plays a predominant role in the pathogen-induced SA biosynthesis in Arabidopsis (Wildermuth et al, Nature, 2001; Garcion et al, Plant Physiology, 2008). In agreement with this, the RipE1-triggered overexpression of *AtPR1* in Arabidopsis correlates with an enhanced expression of *AtICS1*, but not *AtPAL1*. However, it seems that the RipE1-induced increase in SA content in *N. benthamiana* correlates with a reduction of *NbICS1* gene expression, and an increase in the expression of several *NbPAL* genes. Considering that ICS1 is normally regulated at the transcriptional level upon pathogen perception (Wildemurth et al, 2001), our results suggest that the PAL pathway is more relevant than the ICS pathway for the induction of RipE1-triggered immunity in *N. benthamiana*, indicating that both pathways are differentially required for distinct immune responses in different plant species. Similarly, both the ICS and PAL pathways have been reported to be required for pathogen-induced SA biosynthesis in soybean (Shine et al, New Phytol, 2016). The reduction in ICS1 expression in *N. benthamiana* may reflect a compensatory effect between the ICS and PAL pathway. In addition to different gene expression patterns, the physiological output in both plant species may be different. Although RipE1 expression caused an inhibition of Arabidopsis growth, we did not observe any signs of cell death (data not shown), which contrasts with our observation in *N. benthamiana*. However, this may be caused by differences in the expression system used in both plants (Agrobacterium-mediated transient expression in *N. benthamiana vs* EST-induced expression in Arabidopsis stable transgenic plants).

Another surprising aspect of RipE1-triggered immunity is the fact that it leads to the simultaneous accumulation of SA and JA, and to a strong and moderate SA- and JA-triggered gene expression, respectively, in both *N. benthamiana* and Arabidopsis. This suggests that, in the case of RipE1-triggered immunity, SA and JA may play a cooperative role, possibly reflecting the complexity of the *R. solanacearum* infection

process compared to other pathogens.

If RipE1 triggers immunity in *N. benthamiana*, why is it that a GMI1000 strain without PopP1 and AvrA (but having RipE1) can cause a successful infection in *N. benthamiana* without triggering immunity (Poueymiro et al, 2009)? Here, we found that other effectors within GMI1000, such as RipAY, are able to inhibit RipE1-triggered immunity. Since RipE1 perception correlates with an enhancement of cellular glutathione, and RipAY requires its gamma-glutamyl cyclotransferase activity to inhibit RipE1-triggered HR, the degradation of glutathione or other gamma-glutamyl compounds (Sang et al, 2016; Mukaihara et al, 2016; Fujiwara et al, 2016) is the most likely mechanism for this inhibition. Besides RipAY, other T3Es within GMI1000 likely contribute to the suppression of RipE1-triggered HR by targeting other immune functions (Yu et al, bioRxiv, 2019; Wang & Macho, unpublished data). This reflects bacterial adaptation: RipE1 could be important for virulence, but also triggers immunity. In this context, instead of losing RipE1, *R. solanacearum* has developed other effectors to suppress the induction of immunity, while keeping RipE1 virulence activity. Similarly, although transient expression of HopX from *P. syringae* pv *tomato* (*Pto*) triggers HR in specific Arabidopsis accessions, it does not trigger an HR in the context of *Pto* infection (Nimchuk et al, 2007). It is possible that, as in the case of RipE1, the immune responses triggered by HopX are masked during *Pto* infection (as suggested in Nimchuk et al, 2007), likely due to the suppression by other effectors within the same strain.

Materials and Methods

Plant materials and growth conditions

N. benthamiana plants were grown on soil at one plant per pot in an environmentally controlled growth room at 25 ºC under a 16-h light/8-h dark photoperiod with a light-intensity of 130 mE $m^{-2}s^{-1}$. *A. thaliana* plants were grown under the same conditions as *N. benthamiana* for seeds collection. For bacteria virulence and ROS burst assays, *A. thaliana* plants were grown in a growth chamber controlled at 22°C with a 10 h photoperiod and a light-intensity of 100-150 mE $m^{-2}s^{-1}$. After *R. solanacearum* inoculation, Arabidopsis plants were transferred to a growth chamber 27°C with 75% humid under a 12-h light/12-h dark photoperiod.

Chemicals

The flg22 peptide (TRLSSGLKINSAKDDAAGLQIA) was purchased from Abclonal, USA. All other chemicals were purchased from Sigma-Aldrich unless otherwise

Plasmids, bacterial strains and cultivation conditions

R. solanacearum GMI1000 was grown on solid BG medium plates or cultivated over-night in liquid BG medium at 28°C (Morel et al., 2018). The *ripE1* gene from *R. solanacearum* GMI1000 cloned in pDonor207 (donated by Nemo Peeters and Anne-Claire Cazale) was subcloned into pGWB505 by LR reaction (ThermoFisher, USA) to generate a fusion protein with eGFP tag at the C-terminal (Nakagawa *et al.*, 2007). *RipE1* and *ripE1* mutants were inserted between BamH1 and Xho1 restriction sites on sXVE:GFPc:Bar estradiol inducible vector using enzyme digestion (Schlücking et al., 2013). These generated binary vectors were transformed into *Agrobacterium tumefaciens* (Agrobacterium) *GV3101 f*or transient or stable gene expression in *N. benthamiana* and *A. thaliana* plants. Agrobacterium carrying pGWB505 vectors were grown at 29°C and 220 rpm in LB medium supplemented with rifampicin 50 mg/l, gentamycin 25 mg/l and spectinomycin 50 mg/l, while those carrying estradiol inducible vectors were grown in rifampicin 50 mg/l, gentamycin 25

mg/l and kanamycin 50 mg/l.

Site-directed mutagenesis

RipE1$_{C172A}$ and *RipE1 ΔAD* mutant variants were generated using the QuickChange Lightning Site-Directed Mutagenesis Kit (Life technologies, USA) following the manufacturer's instructions. RipE1/pDONR207 plasmid was used as template. Primers used for the mutagenesis are listed in Table S1.

Agrobacterium-mediated gene expression in *A. thaliana and N. benthamiana*

Stable transgenic Arabidopsis plants with *RipE1* and *RipE1* mutated variants driven by estradiol inducible promoter were obtained using the floral dip method (Zhang et. al, 2006). Homozygous T_3 lines were used for all the experiments. Agrobacterium-mediated transient expression in *N. benthamiana* was performed as described (Li, 2011). Agrobacterium carrying the resultant plasmids were suspended in infiltration buffer to a final $OD_{600\ of}$ 0.1~0.5 and infiltrated into the abaxial side of the leaves using the 1mL needless syringe. Leaf samples were taken at 1-3 dpi (days post infiltration) for analysis based on experimental requirements.

Protein extraction and western blots

Plant tissues were collected into 2 ml tubes with metal beads and frozen in liquid nitrogen. After grinding with a tissue lyser (Qiagen, Germany) for 1 min at 30 rpm/s, proteins were extracted using protein extraction buffer (100 mM Tris-HCl pH 8, 150 mM NaCl, 10% glycerol, 5 mM Ethylene diamine tetra acetic acid (EDTA), 2 mM Dithiothreitol (DTT), 1x Plant Protease Inhibitor cocktail, 1% NP-40, 2 mM Phenylmethylsulfonyl fluoride (PMSF), 10 mM Na_2MoO_4, 10 mM NaF, 2 mM Na_3VO_4) and incubating for 5 min. After centrifugation, the supernatants were mixed with SDS loading buffer, incubated at 70 ºC for 10 min, and resolved using SDS-PAGE. Proteins were transferred to a PVDF membrane and monitored by western blot using anti-GFP (Abicode, M0802-3a) and anti-luciferase (Sigma, L0159) antibodies.

421 **Measurement of ROS generation and MAPK activation**

422 PAMP-triggered ROS burst and MAPK activation in plant leaves were measured as
423 described previously (Sang et al., 2017; Segonzac *et al.*, 2011). ROS was elicited with
424 50 nM flg22. MAPK activation assays were performed using 4 to 5-week-old *N.*
425 *benthamiana*. Two days after Agrobacterium infiltration at OD_{600} of 0.1, the intact
426 leaves were elicited for 15 min after vacuum infiltration of 100nM pto-flg22. Leaf discs
427 were taken to monitor MAPK activation by western blot with Phospho-p44/42 MAPK
428 (Erk1/2; Thr-202/Tyr-204) antibodies.

429

430 **Cell death measurement**

431 Cell death in plant leaves was quantified as previously described (Yu et al, bioRxiv,
432 2019) by measuring the electrolyte leakage using a conductivity meter (ThermoFisher,
433 USA) or observing the autofluorescence using the BioRad Gel Imager (Bio-Rad, USA).
434 Briefly, one day after Agrobacterium infiltration in *N. benthamiana*, one 13 mm leaf
435 disk was immersed in 4 mL of distilled water for 1 h with gentle shaking and then
436 transferred to a 6-well culture plate containing 4 mL distilled water in each well. The
437 ion conductivity was then measured at different time intervals. Autofluorescence in
438 intact *N. benthamiana* leaves was measured at 2.5 dpi.

439

440 **RNA isolation and qRT-PCR**

441 Total RNA was extracted using the E.Z.N.A. Plant RNA kit with DNA digestion on
442 column (Biotek, China) according to the manufacturer's instructions. RNA samples
443 were quantified with a Nanodrop spectrophotometer (ThermoFisher, USA). First
444 strand cDNA was synthesized using the iScript^{TM} cDNA synthesis kit (Bio-Rad).
445 qRT-PCR was performed using the iTaq^{TM} Universal SYBR Green Supermix (Bio-Rad)
446 and CFX96 Real-time system (Bio-Rad) and the qPCR data was analyzed as
447 described by (Livak & Schmittgen, 2001). Primers for qPCR of SA-JA related genes in
448 *N. benthamiana* were used as described by Nakano and Mukaihara (2018). Primer
449 sequences are listed in Table S1.

450

Measurements of SA and JA content in plant leaves

SA and JA content were quantified using the method described by Forcat and collaborators (2008) with the following modifications. Leaves (50 mg FW) were collected 42 hours after Agrobacterium infiltration and frozen in liquid nitrogen before grounding into fine powder with the Qiagen tissue lyser. SA and JA were extracted at 10□C for 1 h using 70% methanol extraction solvent spiked with d4-SA as internal standards. Supernatant was taken after centrifuge at 20000 rcf for 10 min and analyzed on ACQUITY UPLC I-class coupled with AB SCIEX TripleTOF 5600+. Analytical column is ACQUITY UPLC BECH C18 1.7 μm, 2.1X150 mm column. The JA concentration was calculated based on the calibration curve created by running JA standard solution. The results were analyzed by peakview1.2.

Measurements of total cellular glutathione in *N. benthamiana* leaves

Total cellular glutathione was measured as previously described (Sang et al, 2016). Briefly, 10 mg of *N. benthamiana* leaves were collected and glutathione was measured using a Glutathione Assay Kit (Beyotime, China) according to the manufacturer's instructions.

Virus-induced gene silencing (VIGS) in *N. benthamiana*

VIGS in *N. benthamiana* plants was performed using TRV vectors as described (Senthil-Kumar & Mysore, 2014). VIGS of *NbSGT1* was performed with several modifications described by Yu and collaborators (2019). Cultures of Agrobacterium carrying pTRV2:*NbSGT1* plasmids or pTRV2 plasmids were mixed at 1:1 ratio and co-infiltrated into the lower leaves of 3-week-old *N. benthamiana* plants. The upper leaves were used for experimental assay within 7-10 days after VIGS application. Silencing of NRCs (NLR required for cell death) in *N. benthamiana* and subsequent expression of T3Es was performed as described by Wu and collaborators (2017).

***Ralstonia solanacearum* virulence assay**

Four week-old *A. thaliana* plants, grown in Jiffy pots, were inoculated with *R. solanacearum* without wounding by soil drenching. An overnight-grown bacterial suspension was diluted to obtain an inoculum of 5.10^7 cfu/ml. Once the Jiffy pots were completely drenched, the plants were removed from the bacterial solution and placed back on a bed of potting mixture soil. The genotypes to be tested were placed in a random order in order to allow an unbiased analysis of the wilting. Daily scoring of the visible wilting on a scale ranging from 0 to 4 (or 0 to 100% leaves wilting), led to an analysis using the Kaplan-Meier survival analysis, log-rank test and hazard ratio calculation as previously described (Morel et al., 2018)

Acknowledgements

We thank Nemo Peeters and Anne-Claire Cazale for sharing unpublished biological materials, Chanhong Kim and Brian Staskawicz for sharing biological materials, Rosa Lozano-Duran for critical reading of this manuscript, and Xinyu Jian for technical and administrative assistance during this work. We thank the PSC Cell Biology, Proteomics, and Metabolomics core facilities for assistance with confocal microscopy and mass spectrometry analysis, respectively. This work was supported by the Strategic Priority Research Program of the Chinese Academy of Sciences (grant XDB27040204), the National Natural Science Foundation of China (NSFC; grant 31571973), the Chinese 1000 Talents Program, and the Shanghai Center for Plant Stress Biology (Chinese Academy of Sciences). The authors have no conflict of interest to declare.

References

Azevedo, C., Sadanandom, A., Kitagawa, K., Freialdenhoven, A., Shirasu, K., and Schulze-Lefert, P. (2002). The RAR1 interactor SGT1, an essential component of *R* gene-triggered disease resistance. Science 295:2073-2076.

Bell E, Creelman RA, Mullet JE. (1995). A chloroplast lipoxygenase is required for wound-induced jasmonic acid accumulation in Arabidopsis. Proceedings of the National Academy of Sciences, USA 92: 8675–8679.

Burger, M., and Chory, J. (2019). Stressed out about hormones: how plants orchestrate immunity. Cell Host Microbe 26:163-172.

Catherine, D., Yves, M., Nicolas, D., Marine, C., Patrick, D., Philippe, R., Yves, M., Alain, J., and Deborah, G. (2012). Deciphering the route of *Ralstonia solanacearum* colonization in *Arabidopsis thaliana* roots during a compatible interaction: focus at the plant cell wall. Planta 236:1419-1431.

Chiang, Y.-H., and Coaker, G. (2015). Effector Triggered Immunity: NLR immune perception and downstream defense responses. The Arabidopsis Book 2015.

Clarke, C.R., Studholme, D.J., Byron, H., Brendan, R., Alexandra, W., Rongman, C., Tadeusz, W., Marie-Christine, D., Emmanuel, W., and Castillo, J.A. (2015). Genome-enabled phylogeographic investigation of the quarantine pathogen *Ralstonia solanacearum* Race 3 Biovar 2 and screening for sources of resistance against its core effectors. Phytopathology 105:597-607.

Cui, H., Tsuda, K., Parker, J.E. (2015). Effector-triggered immunity: from pathogen perception to robust defense. In: Annual Review Plant Biology. 487-511.

Delaney, T.P., Uknes, S., Vernooij, B., Friedrich, L., Weymann, K., Negrotto, D., Gaffney, T., Gut-Rella, M., Kessmann, H., and Ward, E. (1994). A central role of salicylic acid in plant disease resistance. Science 266:1247-1250.

Forcat, S., Bennett, M., Mansfield, J., and Grant, M. (2008). A rapid and robust method for simultaneously measuring changes in the phytohormones ABA, JA and SA in plants following biotic and abiotic stress. Plant methods 4:16.

Fujiwara, S., Kawazoe, T., Ohnishi, K., Kitagawa, T., Popa, C., Valls, M., Genin, S., Nakamura, K., Kuramitsu, Y., and Tanaka, N. (2016). RipAY, a plant pathogen effector protein exhibits robust γ-glutamyl cyclotransferase activity when stimulated by eukaryotic thioredoxins. Journal of Biological Chemistry 291:6813.

Galán, J.E., Lara-Tejero, M., Marlovits, T.C., and Wagner, S. (2014). Bacterial type III secretion systems: specialized nanomachines for protein delivery into target cells. Annual Review of Microbiology 68:415.

Garcion, C., Lohmann, A., Lamodière, E., Catinot, J., Buchala, A., Doermann, P., and Métraux, J.-P. (2008). Characterization and biological function of the ISOCHORISMATE SYNTHASE2 gene of Arabidopsis. Plant Physiology 147:1279-1287.

Gassmann, W., ., Hinsch, M.E., and Staskawicz, B.J. (2010). The Arabidopsis RPS4 bacterial-resistance gene is a member of the TIR-NBS-LRR family of

553 disease-resistance genes. Plant Journal for Cell & Molecular Biology
554 20:265-277.
555 Gimenez-Ibanez, S., Boter, M., Fernández-Barbero, G., Chini, A., Rathjen, J.P., and
556 Solano, R. (2014). The bacterial effector HopX1 targets JAZ transcriptional
557 repressors to activate jasmonate signaling and promote infection in
558 Arabidopsis. PLoS Biology 12:e1001792-e1001792.
559 Jayaraman, J., Segonzac, C., Cho, H., Jung, G., and Sohn, K.H. (2016).
560 Effector-assisted breeding for bacterial wilt resistance in horticultural crops.
561 Horticulture Environment & Biotechnology 57:415-423.
562 Jiang, G., Wei, Z., Xu, J., Chen, H., Zhang, Y., She, X., Macho, A.P., Ding, W., and
563 Liao, B. (2017). Bacterial wilt in China: history, current status, and future
564 perspectives. Frontiers in Plant Science 8:1549.
565 Jones, J.D.G., and Dangl, J.L. (2006). The plant immune system. Nature
566 444:323-329.
567 Kadota, Y., Shirasu, K., and Guerois, R. (2010). NLR sensors meet at the
568 SGT1–HSP90 crossroad. Trends in biochemical sciences 35:199-207.
569 Lavie, M., Shillington, E., Eguiluz, C., Grimsley, N., and Boucher, C. (2002). PopP1, a
570 new member of the YopJ/AvrRxv family of type III effector proteins, acts as a
571 host-specificity factor and modulates aggressiveness of *Ralstonia*
572 *solanacearum*. Molecular plant-microbe interactions : MPMI 15:1058.
573 Leroux, C., Huet, G., Jauneau, A., Camborde, L., Trémousaygue, D., Kraut, A., Zhou,
574 B., Levaillant, M., Adachi, H., and Yoshioka, H. (2015). A receptor pair with an
575 integrated decoy converts pathogen disabling of transcription factors to
576 immunity. Cell 161:1074-1088.
577 Li, X. (2011). Infiltration of *Nicotiana benthamiana* protocol for transient expression via
578 Agrobacterium. Bio-protocol Bio101:e95.
579 Livak, K.J., and Schmittgen, T.D. (2001). Analysis of relative gene expression data
580 using real-time quantitative PCR and the 2(-Delta Delta C(T)) Method.
581 Methods 25:402-408.
582 Macho, A.P. (2016). Subversion of plant cellular functions by bacterial type-III
583 effectors: beyond suppression of immunity. New Phytologist 210:51-57.
584 Macho, A.P., and Zipfel, C. (2015). Targeting of plant pattern recognition
585 receptor-triggered immunity by bacterial type-III secretion system effectors.
586 Current Opinion in Microbiology 23:14-22.
587 Makarova, K.S., Aravind, L., and Koonin, E.V. (1999). A superfamily of archaeal,
588 bacterial, and eukaryotic proteins homologous to animal transglutaminases.
589 Protein Science 8:1714-1719.
590 Manifield, John, GENIN, Stephane, MAGORI, Shimpei, CITOVSKY, Vitaly, and
591 SRIARIYANUM. (2012). Top 10 plant pathogenic bacteria in molecular plant
592 pathology. Molecular Plant Pathology 13:614-629.
593 Mansfield, J., Jenner, C., Hockenhull, R., Bennett, M.A., and Stewart, R. (1994).
594 Characterization of avrPphE, a gene for cultivar-specific avirulence from
595 *Pseudomonas syringae* pv. *phaseolicola* which is physically linked to hrpY, a

new hrp gene identified in the halo-blight bacterium. Molecular Plant Microbe Interaction 7:726-739.

Morel A, G.J., Lonjon F, Sujeeun L, Barberis P, Genin S, Vailleau F, Daunay MC, Dintinger J, Poussier S, Peeters N, Wicker E. (2018). The eggplant AG91-25 recognizes the Type III-secreted effector RipAX2 to trigger resistance to bacterial wilt (*Ralstonia solanacearum* species complex). Molecular Plant Pathology 19:13.

Morel, A., Peeters, N., Vailleau, F., Barberis, P., Jiang, G., Berthomé, R., and Guidot, A. (2018). Plant pathogenicity phenotyping of *Ralstonia solanacearum* strains. in: Host-Pathogen Interactions: Methods and Protocols--Medina, C., and López-Baena, F.J., eds. New York, NY: Springer New York. 223-239.

Mukaihara, T., Hatanaka, T., Nakano, M., and Oda, K. (2016). *Ralstonia solanacearum* Type III effector RipAY is a glutathione-degrading enzyme that is activated by plant cytosolic thioredoxins and suppresses plant immunity. Mbio 7:e00359.

Mukaihara, T., Tamura, N., and Iwabuchi, M. (2010). Genome-wide identification of a large repertoire of *Ralstonia solanacearum* type III effector proteins by a new functional screen. Molecular Plant Microbe Interaction 23:251-262.

Nahar, K., Matsumoto, I., Taguchi, F., Inagaki, Y., Yamamoto, M., Toyoda, K., Shiraishi, T., Ichinose, Y., and Mukaihara, T. (2014). *Ralstonia solanacearum* type III secretion system effector Rip36 induces a hypersensitive response in the nonhost wild eggplant *Solanum torvum*. Molecular Plant Pathology 15:297-303.

Nakagawa, T., Suzuki, T., Murata, S., Nakamura, S., Hino, T., Maeo, K., Tabata, R., Kawai, T., Tanaka, K., and Niwa, Y. (2007). Improved Gateway binary vectors: high-performance vectors for creation of fusion constructs in transgenic analysis of plants. Journal of the Agricultural Chemical Society of Japan 71:2095-2100.

Nakano M, M.T. (2019). The type III effector RipB from *Ralstonia solanacearum* RS1000 acts as a major avirulence factor in *Nicotiana benthamiana* and other Nicotiana species. Mol Plant Pathol 20:14.

Nakano, M., and Mukaihara, T. (2018). *Ralstonia solanacearum* Type III effector RipAL targets chloroplasts and induces jasmonic acid production to suppress salicylic acid-mediated defense responses in plants. Plant and Cell Physiology 59:2576-2589.

Nimchuk, Z.L., Fisher, E.J., Desveaux, D., Chang, J.H., and Dangl, J.L. (2007). The HopX (AvrPphE) family of *Pseudomonas syringae* type III effectors require a catalytic triad and a novel N-terminal domain for function. Molecular plant-microbe interactions : MPMI 20:346.

Peeters, N., Carrère, S., Anisimova, M., Plener, L., Cazalé, A.C., and Genin, S. (2013a). Repertoire, unified nomenclature and evolution of the Type III effector gene set in the *Ralstonia solanacearum* species complex. BMC Genomics 14:859-859.

639 Peeters, N., Guidot, A., Vailleau, F., and Valls, M. (2013b). *Ralstonia solanacearum*, a
640 widespread bacterial plant pathogen in the post-genomic era. Molecular Plant
641 Pathology 14:651–662.
642 Poueymiro, M., Cunnac, S., Barberis, P., Deslandes, L., Peeters, N., Cazale-Noel,
643 A.C., Boucher, C., and Genin, S. (2009). Two type III secretion system
644 effectors from *Ralstonia solanacearum* GMI1000 determine host-range
645 specificity on tobacco. Molecular Plant Microbe Interaction 22:538-550.
646 Rosas-Díaz, T., Cana-Quijada, P., Amorim-Silva, V., Botella, M.A., Lozano-Durán, R.,
647 and Bejarano, E.R. (2017). *Arabidopsis NahG* plants as a suitable and efficient
648 system for transient expression using *Agrobacterium tumefaciens*. Molecular
649 Plant 10:353-356.
650 Sang, Y., and Macho, A.P. (2017). Analysis of PAMP-triggered ROS burst in plant
651 immunity. Methods in Molecular Biology 1578:143.
652 Sang, Y., Wang, Y., Ni, H., Cazalã, A.C., She, Y.M., Peeters, N., and Macho, A.P.
653 (2016). The *Ralstonia solanacearum* type III effector RipAY targets plant redox
654 regulators to suppress immune responses. Molecular Plant Pathology 19.
655 Sarris, P., Duxbury, Z., Huh, S.U., Ma, Y., Segonzac, C., Sklenar, J., Derbyshire, P.,
656 Cevik, V., Rallapalli, G., and Saucet, S. (2015). A plant immune receptor
657 detects pathogen effectors that target WRKY transcription factors. Cell
658 161:1089-1100.
659 Schlücking, K., Kai, H.E., Köster, P., Drerup, M.M., Eckert, C., Steinhorst, L., Waadt,
660 R., Batistič, O., and Kudla, J. (2013). A new β-estradiol-inducible vector set
661 that facilitates easy construction and efficient expression of transgenes
662 reveals CBL3-dependent cytoplasm to tonoplast translocation of CIPK5.
663 Molecular Plant 6:1814-1829.
664 Schultink, A., Qi, T., Lee, A., Steinbrenner, A.D., and Staskawicz, B. (2017). Roq1
665 mediates recognition of the Xanthomonas and Pseudomonas effector proteins
666 XopQ and HopQ1. Plant Journal 92.
667 Segonzac, C., Feike, D., Gimenez Ibanez, S., Dagmar R, H., Zipfel, C., and John P,
668 R. (2011). Hierarchy and roles of pathogen-associated molecular
669 pattern-induced responses in Nicotiana benthamiana. Plant Physiology
670 156:687-699.
671 Senthil-Kumar, M., and Mysore, K.S. (2014). Tobacco rattle virus–based
672 virus-induced gene silencing in *Nicotiana benthamiana*. Nature Protocols
673 9:1549.
674 Shine, M.B., Yang, J.W., El-Habbak, M., Nagyabhyru, P., Fu, D.Q., Navarre, D.,
675 Ghabrial, S., Kachroo, P., and Kachroo, A. (2016). Cooperative functioning
676 between phenylalanine ammonia lyase and isochorismate synthase activities
677 contributes to salicylic acid biosynthesis in soybean. New Phytologist
678 212:627-636.
679 Solé, M., Popa, C., Mith, O., Sohn, K.H., Jones, J., Deslandes, L., and Valls, M.
680 (2012). The awr gene family encodes a novel class of *Ralstonia solanacearum*

type III effectors displaying vrulence and avirulence activities. Molecular plant-microbe interactions : MPMI 25:941-953.

Stevens, C., Bennett, M.A., Athanassopoulos, E., Tsiamis, G., Taylor, J.D., and Mansfield, J.W. (1998). Sequence variations in alleles of the avirulence gene avrPphE.R2 from *Pseudomonas syringae* pv. *phaseolicola* lead to loss of recognition of the AvrPphE protein within bean cells and a gain in cultivar-specific virulence. Molecular Microbiology 29:165-177.

Tasset, C., Bernoux, M., Jauneau, A., Pouzet, C., Brière, C., Kieffer-Jacquinod, S., Rivas, S., Marco, Y., and Deslandes, L. (2010). Autoacetylation of the *Ralstonia solanacearum* effector PopP2 targets a lysine residue essential for RRS1-R-mediated immunity in Arabidopsis. PLOS Pathogens 6:e1001202.

Turner, M., Jauneau, A., Genin, S., Tavella, M.J., Vailleau, F., Gentzbittel, L., and Jardinaud, M.F. (2009). Dissection of bacterial wilt on *Medicago truncatula* revealed two type III secretion system effectors acting on root infection process and disease development. Plant Physiology 150:1713-1722.

Vlot, A.C., Dempsey, D.M.A., and Klessig, D.F. (2009). Salicylic acid, a multifaceted hormone to combat disease. Annual Review of Phytopathology 47:177-206.

Ward, E.R., Uknes, S.J., Williams, S.C., Dincher, S.S., Wiederhold, D.L., Alexander, D.C., Ahlgoy, P., Métraux, J.P., and Ryals, J.A. (1991). Coordinate gene activity in response to agents that induce systemic acquired resistance. Plant Cell 3:9.

Wei, Y., Caceres-Moreno, C., Jimenez-Gongora, T., Wang, K., Sang, Y., Lozano-Duran, R., and Macho, A.P. (2017). The *Ralstonia solanacearum* csp22 peptide, but not flagellin-derived peptides, is perceived by plants from the Solanaceae family. Plant Biotechnology Journal 16.

Wiermer, Marcel, FEYS, Bart, J., PARKER, and Jane, E. (2005). Plant immunity : the EDS1 regulatory node. Current Opinion in Plant Biology 8:383-389.

Wildermuth, M.C., Dewdney, J., ., Wu, G., ., and Ausubel, F.M. (2001). Isochorismate synthase is required to synthesize salicylic acid for plant defence. Nature 414:562-565.

Williams, S.J., Kee Hoon, S., Li, W., Maud, B., Sarris, P.F., Cecile, S., Thomas, V., Yan, M., Saucet, S.B., and Ericsson, D.J. (2014). Structural basis for assembly and function of a heterodimeric plant immune receptor. Science 344:299-303.

Wu, C.-H., Abd-El-Haliem, A., Bozkurt, T.O., Belhaj, K., Terauchi, R., Vossen, J.H., and Kamoun, S. (2017). NLR network mediates immunity to diverse plant pathogens. Proceedings of the National Academy of Sciences USA 114:8113-8118.

Wu, C.H., Belhaj, K., Bozkurt, T.O., Birk, M.S., and Kamoun, S. (2016). Helper NLR proteins NRC2a/b and NRC3 but not NRC1 are required for Pto-mediated cell death and resistance in *Nicotiana benthamiana*. New Phytologist 209:1344-1352.

723 Yu, G., Xian, L., Sang, Y., and Macho, A.P. (2019a). Cautionary notes on the use of
724 Agrobacterium-mediated transient gene expression upon SGT1 silencing in
725 *Nicotiana benthamiana*. New Phytologist 222:14-17.
726 Yu, G., Xian, L., Xue, H., Yu, W., Rufian, J., Sang, Y., Morcillo, R., Wang, Y., and
727 Macho, A.P. (2019b). A bacterial effector protein prevents MAPK-mediated
728 phosphorylation of SGT1 to suppress plant immunity. bioRxiv:641241.
729 Zhang, X., Henriques, R., Lin, S.-S., Niu, Q.-W., and Chua, N.-H. (2006).
730 Agrobacterium-mediated transformation of *Arabidopsis thaliana* using the
731 floral dip method. Nature Protocols 1:641.
732

Figure legends

Figure 1. RipE1 triggers cell death in *Nicotiana benthamiana*.

(a) RipE1-GFP or GFP (as control) were expressed in the same leaf of *N. benthamiana* using Agrobacterium with an OD_{600} of 0.5. Photos were taken 2 days post-inoculation with a CCD camera (upper panel) or an UV camera (lower panel). UV signal corresponds to the development of cell death (not GFP fluorescence). UV images were taken from the abaxial side and flipped horizontally for representation. (b) Ion leakage measured in leaf discs taken from *N. benthamiana* tissues expressing RipE1-GFP or GFP (as control), representative of cell death, at the indicated timepoints. Values indicate mean ± SE (n=3). (c) Simplified diagram of RipE1, including the residues comprising the Domain A and the predicted catalytic triad. (d) Western blot showing the accumulation of RipE1 mutant variants. ΔAD corresponds to a deletion mutant of the Domain A (residues 121-128). Molecular weight (kDa) marker bands are indicated for reference. (e) Cell death triggered by RipE1 mutant variants (conditions as in (a)). (f) Ion leakage measured in leaf discs taken from *N. benthamiana* tissues expressing RipE1 mutant variants (conditions as in (b). Each experiment was repeated at least 3 times with similar results.

Figure 2. RipE1 activates SA-dependent immune responses in *N. benthamiana*.

(a) Quantitative RT-PCR to determine the expression of RipE1 and *NbPR1* in *N. benthamiana* tissues expressing GFP, RipE1, or RipE1 C172A, using Agrobacterium with an OD_{600} of 0.5. Samples were taken at the indicated times after Agrobacterium infiltration. In each case, the RipE1 variants and their respective GFP control were expressed in the same leaf, and values are represented side-by-side. Expression values are relative to the expression of the housekeeping gene *NbEF1a*. Values indicate mean ± SE (n=3). (b-d) RipE1-Nluc was co-expressed with GFP (as control) or with NahG-GFP in the same leaf. Protein accumulation is shown in the figure S3. (b) Photos were taken 2.5 days post-inoculation with a CCD camera (upper panel) or an UV camera (lower panel). UV signal corresponds to the development of cell death (not GFP fluorescence). UV images were taken from the abaxial side and flipped

763 horizontally for representation. (c) Ion leakage measured in leaf discs taken from *N.*
764 *benthamiana* tissues expressing RipE1 together with GFP or NahG-GFP,
765 representative of cell death, at the indicated timepoints. Values indicate mean ± SE
766 (n=3). (c) Quantitative RT-PCR to determine the expression of *NbPR1* in *N.*
767 *benthamiana* tissues 48 hours after Agrobacterium infiltration. Expression values are
768 relative to the expression of the housekeeping gene *NbEF1a*. Values indicate mean ±
769 SE (n=3). Each experiment was repeated at least 3 times with similar results.
770
771 **Figure 3. RipE1 perception enhances the expression of *PAL* genes and SA**
772 **biosynthesis in *N. benthamiana*.**
773 (a) Measurement of SA accumulation in *N. benthamiana* tissues expressing GFP,
774 RipE1, or RipE1 C172A, using Agrobacterium with an OD_{600} of 0.5. Samples were
775 taken 42 hours after Agrobacterium infiltration. Three independent biological repeats
776 were performed, and the different colors indicate values from different replicates.
777 Values are represented as % of the GFP control in each replicate. (b-f) Quantitative
778 RT-PCR to determine the expression of *NbICS1* (b), *NbPAL05* (c), *NbPAL08* (d),
779 *NbPAL10* (e), and *NbLOX2* (f) in *N. benthamiana* tissues expressing GFP, RipE1, or
780 RipE1 C172A, using Agrobacterium with an OD_{600} of 0.5. Samples were taken at the
781 indicated times after Agrobacterium infiltration. In each case, the RipE1 variants and
782 their respective GFP control were expressed in the same leaf, and values are
783 represented side-by-side. Expression values are relative to the expression of the
784 housekeeping gene *NbEF1a*. Values indicate mean ± SE (n=3). Each experiment was
785 repeated at least 3 times with similar results.
786
787 **Figure 4. RipE1-triggered responses require SGT1, but not EDS1.**
788 (a-d) RipE1-GFP or GFP (as control) were expressed in the same leaf of *N.*
789 *benthamiana* undergoing VIGS of *NbSGT1* or VIGS with an empty vector (EV)
790 construct (as control), using Agrobacterium with an OD_{600} of 0.5. (a) Western blot
791 showing the accumulation of GFP, RipE1-GFP, and endogenous *NbSGT1*. Molecular
792 weight (kDa) marker bands are indicated for reference. Vertical lines next to the bands

are due to the high sensitivity setting used in the imaging equipment. (b) Photos were taken 2 days post-inoculation with a CCD camera (upper panel) or an UV camera (lower panel). UV signal corresponds to the development of cell death (not GFP fluorescence). UV images were taken from the abaxial side and flipped horizontally for representation. (c) Ion leakage measured in leaf discs taken from *N. benthamiana* tissues expressing RipE1-GFP or GFP (as control), representative of cell death, 48 hours after Agrobacterium infiltration. Values indicate mean ± SE (n=3). (d) Quantitative RT-PCR to determine the expression of *NbPR1* in *N. benthamiana* tissues 48 hours after Agrobacterium infiltration. Expression values are relative to the expression of the housekeeping gene *NbEF1a*. Values indicate mean ± SE (n=3). (e) RipE1-GFP or GFP (as control) were expressed in the same leaf of *N. benthamiana* wild type or a stable *eds1* knockout mutant, using Agrobacterium with an OD_{600} of 0.5. Photos were taken 2 days post-inoculation with a CCD camera (upper panel) or an UV camera (lower panel). UV signal corresponds to the development of cell death (not GFP fluorescence). UV images were taken from the abaxial side and flipped horizontally for representation. Each experiment was repeated at least 3 times with similar results.

Figure 5. RipE1 triggers immunity in Arabidopsis.

(a) Arabidopsis Col-0 wild type or independent stable transgenic lines expressing RipE1 or RipE1 C172A from an estradiol (EST)-inducible promoter were grown for 3 weeks and then treated sprayed with 100 µM EST daily. Photographs were taken 2 weeks after beginning the EST treatment. (b) Arabidopsis 4 day-old seedlings were treated with 25 µM EST and samples were taken 1, 2, 3, or 4 days after EST treatment. Quantitative RT-PCR to determine the expression of *RipE1, AtPR1, AtPAL1, AtICS1, AtVSP2,* and *AtPDF1.2*. Expression values are relative to the expression of the housekeeping gene *AtACT2*. Values indicate mean ± SE (n=3). (c) Plants in (a) were inoculated with *R. solanacearum* GMI1000 by soil-drenching. The results are represented as disease progression, showing the average wilting

symptoms in a scale from 0 to 4 (mean ± SEM). n=20 plants per genotype. Each experiment was repeated at least 3 times with similar results.

Figure 6. RipE1-triggered immune responses are suppressed by RipAY.

(a) RipE1-GFP or GFP (as control) were expressed in the same leaf of *N. benthamiana* using Agrobacterium with an OD_{600} of 0.5, and samples were taken at the indicated time points to measure the accumulation of glutathione (GSH). (b-d) RipE1-Nluc was co-expressed with GFP (as control), with RipAY-GFP, or with RipAY-C216A-GFP, respectively, in the same leaf. Protein accumulation is shown in the figure S6. (b) Photos were taken 2.5 days post-inoculation with a CCD camera (upper panel) or an UV camera (lower panel). UV signal corresponds to the development of cell death (not GFP fluorescence). UV images were taken from the abaxial side and flipped horizontally for representation. (c) Ion leakage measured in leaf discs taken from *N. benthamiana* tissues expressing RipE1 together with GFP or NahG-GFP, representative of cell death, at the indicated timepoints. Values indicate mean ± SE (n=3). (c) Quantitative RT-PCR to determine the expression of *NbPR1* in *N. benthamiana* tissues 48 hours after Agrobacterium infiltration. Expression values are relative to the expression of the housekeeping gene *NbEF1a*. Values indicate mean ± SE (n=3). Each experiment was repeated at least 3 times with similar results.

Figure S1. Phylogenetic analysis of RipE1

Alignment of the amino acid sequence of RipE1 from *R. solanacearum* GMI1000 (Rs_RipE1), XopE1 from *Xanthomonas campestris* pv. *vesicatoria* (Xs_XopE1), and HopX1 from *Pseudomonas syringae* pv tabaci 11528 (Ps_HopX1). Residues forming the predicted catalytic triad are indicated in red, and the conserved domain A is indicated in blue. The black shaded amino acids are identical among the three effectors.

Figure S2. RipE1 expression inhibits PTI responses in *N. benthamiana*, which

correlates with the induction of cell death.

Agrobacterium was used to induce the transient expression of RipE1-GFP in half of the leaf and GFP in the other half. (a) Oxidative burst triggered by 50 nM flg22 in *N. benthamiana* tissues at the indicated time points, measured in a luminol-based assay as relative luminescence units (RLU). Values are average ± SE (n=24), and are represented as % of the GFP control in each time point. Western blot with anti-GFP is shown for reference of protein accumulation at each time point. (b) MAPK activation was induced 40 hours after Agrobacterium infiltration with 100 nM flg22 and analysed 15 minutes after flg22 treatment using anti-phosphorylated MAPK antibody (anti-pMAPK). Immunoblots were also analysed using anti-GFP antibody to verify protein accumulation. Anti-actin was used to verify equal loading. Molecular weight (kDa) marker bands are indicated for reference. (c) Oxidative burst was induced as in (a) and measured 2 days post-Agrobacterium infiltration. Mutant variants are described in the Figure 1. (d) Ion leakage was measured as in the Figure 1. Measurement over time after RipE1 expression reflects that the induction of cell death correlates in time with the suppression of PTI responses. The experiments were repeated three times with similar results.

Figure S3. Protein accumulation upon co-expression of RipE1 and NahG.

Western blot showing protein accumulation in the experiments shown in the figure 2. Molecular weight (kDa) marker bands are indicated for reference.

Figure S4. RipE1 expression leads to an increase in JA contents.

Measurement of JA accumulation in *N. benthamiana* tissues expressing GFP or RipE1, using Agrobacterium with an OD_{600} of 0.5. Samples were taken 42 hours after Agrobacterium infiltration. Three independent biological repeats were performed, and the different colors indicate values from different replicates. Values are represented as % of the GFP control in each replicate.

Figure S5. RipE1-triggered cell death does not require NRC proteins.

RipE1-GFP, C172A or GFP (as control) were transiently expressed using agrobacterium into wild type (WT) *N. benthamiana*, leaves silenced with EV (as control) and those silenced with different NRC homologs (NRC2/3, NRC4 and NRC2/3/4-Triple), using VIGS. For RipE1-GFP, C172A and GFP an OD_{600} of 0.5 was used. Rpiblb2 (OD_{600} 0.2)/AVRblb2 (OD_{600} 0.1) and Pto (OD_{600} 0.6)/AVRPto (OD_{600} 0.1), which are NRC4 and NRC2/3 dependent, respectively, were included as controls. Photos were taken 5 days post inoculation under natural or UV light. UV images were taken from the abaxial side and flipped horizontally for representation.

Figure S6. Protein accumulation upon co-expression of RipE1 and RipAY.

Western blot showing protein accumulation in the experiments shown in the figure 6. Molecular weight (kDa) marker bands are indicated for reference.

Table S1: Primers used in this study for RipE1 cloning and qRT-PCR.

Gene	Forward primers	Reverse primers
Primers for site-directed amino acid mutation		
RipE1-C17 2A	AGGGGCGGGGAACGCCGGCGA ACACGCC	GGCGTGTTCGCCGGCGTTCCC CGCCCCT
RipE1 ΔAD	GATACTGACGCACATCGACGCC ACCCA	TGGGTGGCGTCGATGTGCGTCA GTATC
Primers for qRT-PCR in *N. benthamiana*		
NbEF1a	CCCAAGAGGCCCTCAGACA	CACACGACCAACAGGGACAGT
NbPR-1	GGTCAACACGGCGAAAACC	GCCTTAGCAGCCGTCATGA
NbICS1	GTGTCGGCTCTGCTGTCTTCT	CTGCGTATAGCACGCCAATC
NbPAL05	AAGGGAGCTGAAATCGCCAT	TCCGCACTTTGGACATGGTT
NbPAL08	TATCACCCCATGCTTGCCTC	AGTGGCCTTGGAATTGGGTC
NbPAL10	GTCACTCCATGTTTGCCCCT	GACCTGTGAGTAAACCGGCA
NbLOX2	TCTTGGGTGGCTCCTCTGACT	TGTTGGAGGTCTGCCTGTTCT
Primers for qRT-PCR in *A. thaliana*		
AtACTIN2	TGCTGGACGTGACCTTACTG	TTCTCGATGGAAGAGCTGGT
AtPR1	TGATCCTCGTGGGAATTATGT	TGCATGATCACATCATTACTTCA T
AtICS1	GCGTCGTTCGGTTACAGG	ACAGCGAGGCTGAATCTCAT
AtPAL1	TATCCCGAACAGGATCAAGG	TCTCCGGTCAAAAGCTCTGT
AtPDF1.2	ACTATGTCTTCCCAGCACAC	AACAACAACGGGAAAATAAA
AtVSP2	GTTTGGATCTTTGACCTAGACG A	CTCTAACCACGACCAGTACGC
Primers for cloning RipE1 to sXVE:GFPc:Bar estradiol inducible vector		
RipE1	TCAGGATCCATGCCGCCCGTCC TGCCGT	ACTCTCGAGGCTTTCCGTGGCG GGCGGCT

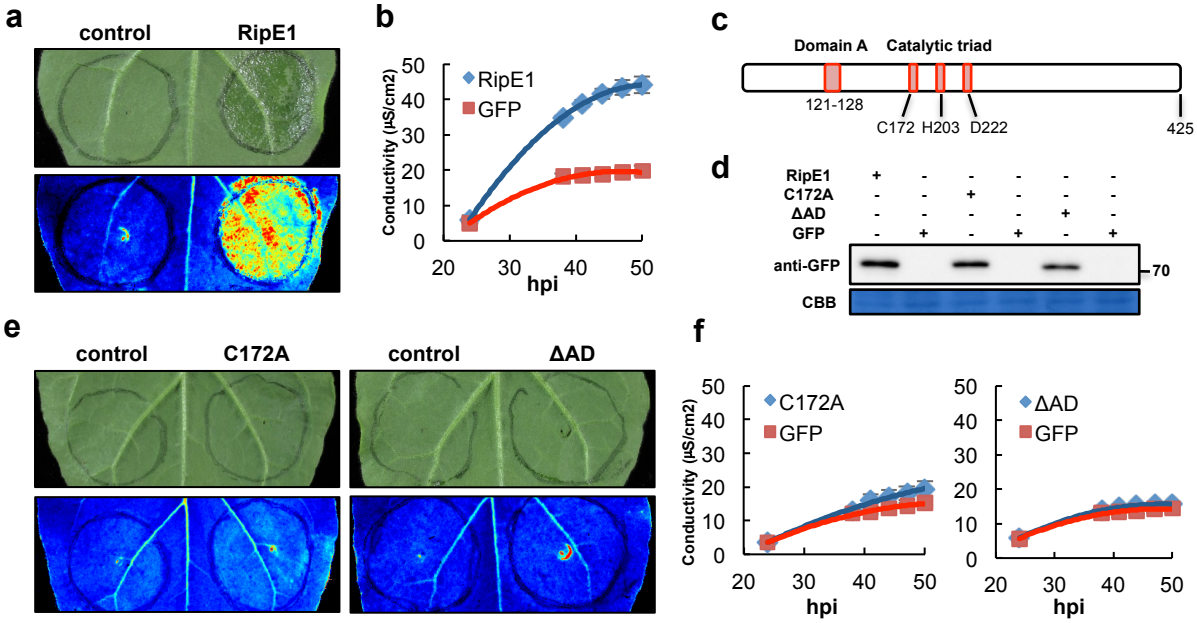

Figure 1. RipE1 triggers cell death in *Nicotiana benthamiana*.
(a) RipE1-GFP or GFP (as control) were expressed in the same leaf of *N. benthamiana* using Agrobacterium with an OD_{600} of 0.5. Photos were taken 2 days post-inoculation with a CCD camera (upper panel) or an UV camera (lower panel). UV signal corresponds to the development of cell death (not GFP fluorescence). UV images were taken from the abaxial side and flipped horizontally for representation. (b) Ion leakage measured in leaf discs taken from *N. benthamiana* tissues expressing RipE1-GFP or GFP (as control), representative of cell death, at the indicated timepoints. Values indicate mean ± SE (n=3). (c) Simplified diagram of RipE1, including the residues comprising the Domain A and the predicted catalytic triad. (d) Western blot showing the accumulation of RipE1 mutant variants. ΔAD corresponds to a deletion mutant of the Domain A (residues 121-128). Molecular weight (kDa) marker bands are indicated for reference. (e) Cell death triggered by RipE1 mutant variants (conditions as in (a)). (f) Ion leakage measured in leaf discs taken from *N. benthamiana* tissues expressing RipE1 mutant variants (conditions as in (b). Each experiment was repeated at least 3 times with similar results.

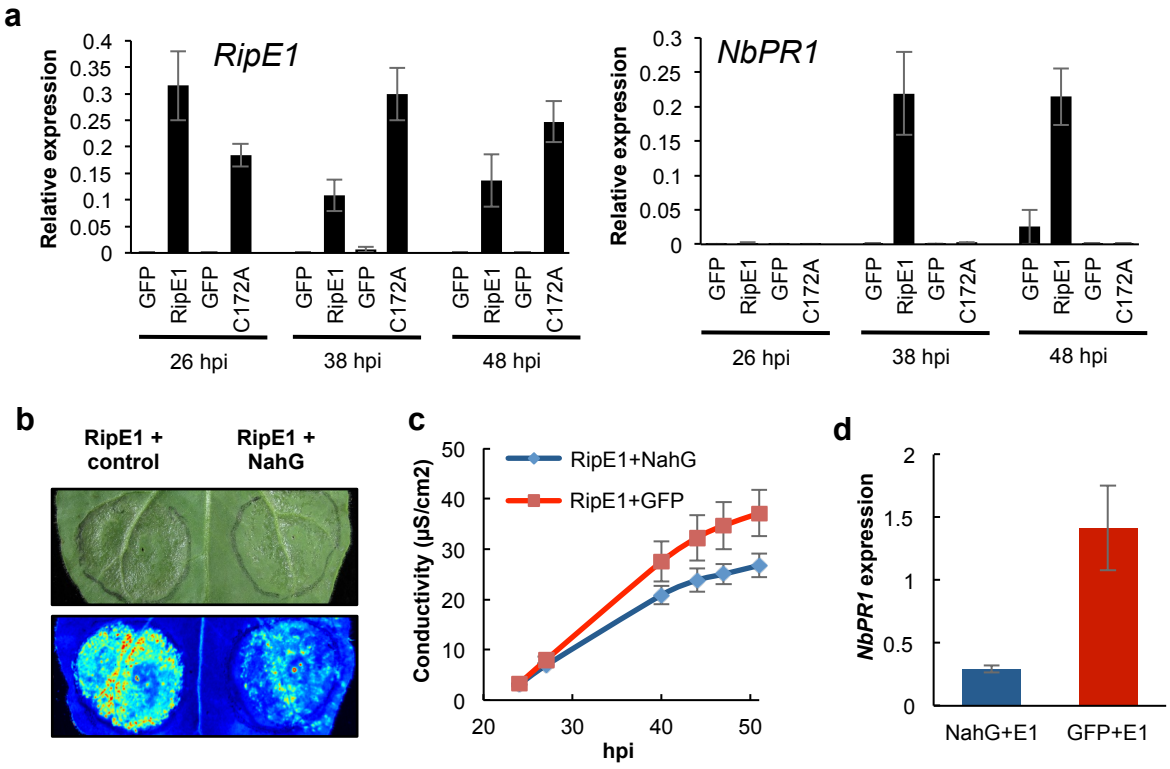

Figure 2. RipE1 activates SA-dependent immune responses in *N. benthamiana*.

(a) Quantitative RT-PCR to determine the expression of RipE1 and *NbPR1* in *N. benthamiana* tissues expressing GFP, RipE1, or RipE1 C172A, using Agrobacterium with an OD_{600} of 0.5. Samples were taken at the indicated times after Agrobacterium infiltration. In each case, the RipE1 variants and their respective GFP control were expressed in the same leaf, and values are represented side-by-side. Expression values are relative to the expression of the housekeeping gene *NbEF1a*. Values indicate mean ± SE (n=3). (b-d) RipE1-Nluc was co-expressed with GFP (as control) or with NahG-GFP in the same leaf. Protein accumulation is shown in the figure S3. (b) Photos were taken 2.5 days post-inoculation with a CCD camera (upper panel) or an UV camera (lower panel). UV signal corresponds to the development of cell death (not GFP fluorescence). UV images were taken from the abaxial side and flipped horizontally for representation. (c) Ion leakage measured in leaf discs taken from *N. benthamiana* tissues expressing RipE1 together with GFP or NahG-GFP, representative of cell death, at the indicated timepoints. Values indicate mean ± SE (n=3). (c) Quantitative RT-PCR to determine the expression of *NbPR1* in *N. benthamiana* tissues 48 hours after Agrobacterium infiltration. Expression values are relative to the expression of the housekeeping gene *NbEF1a*. Values indicate mean ± SE (n=3). Each experiment was repeated at least 3 times with similar results.

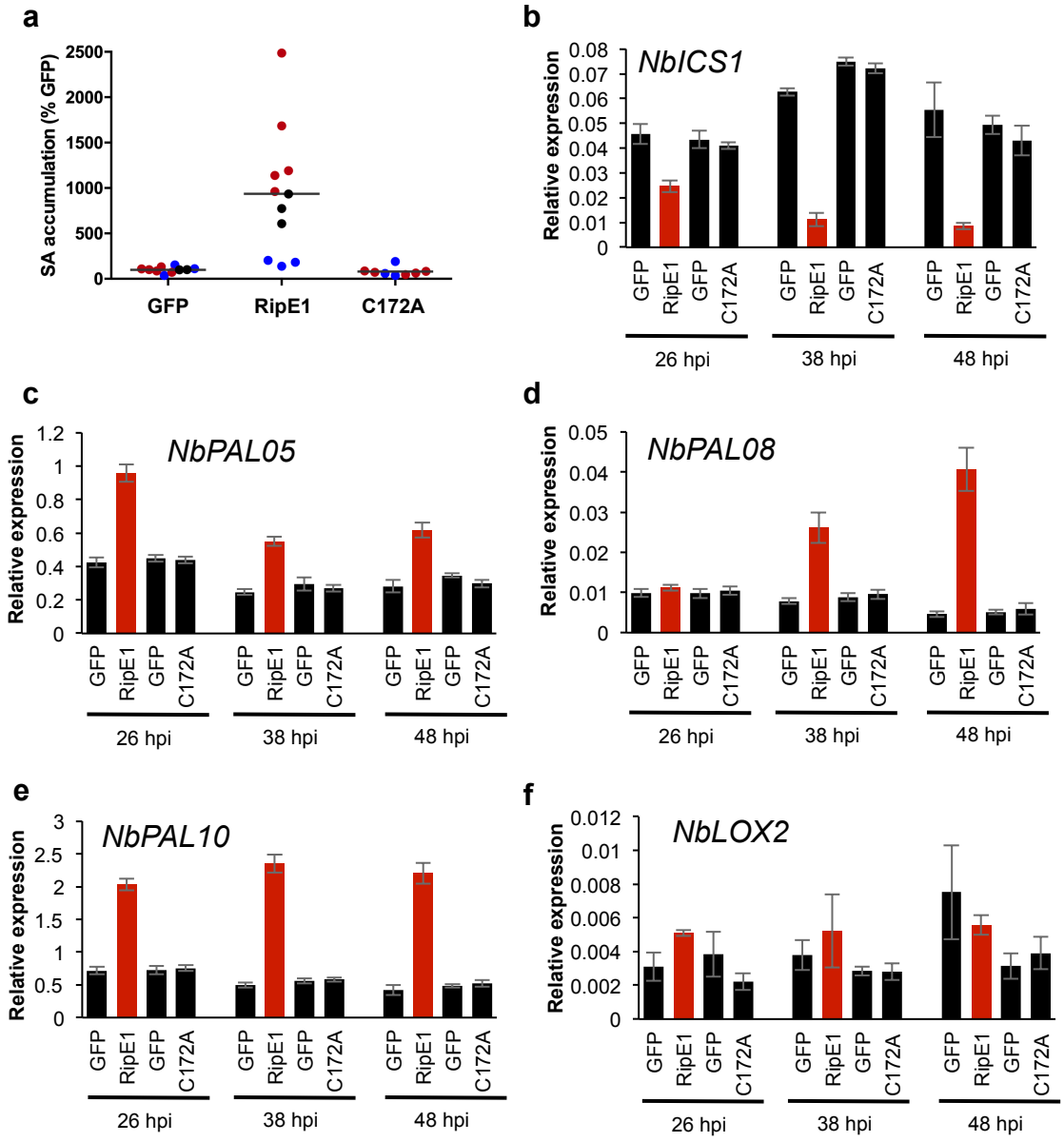

Figure 3. RipE1 perception enhances the expression of *PAL* genes and SA biosynthesis in *N. benthamiana*.

(a) Measurement of SA accumulation in *N. benthamiana* tissues expressing GFP, RipE1, or RipE1 C172A, using Agrobacterium with an OD_{600} of 0.5. Samples were taken 42 hours after Agrobacterium infiltration. Three independent biological repeats were performed, and the different colors indicate values from different replicates. Values are represented as % of the GFP control in each replicate. (b-f) Quantitative RT-PCR to determine the expression of *NbICS1* (b), *NbPAL05* (c), *NbPAL08* (d), *NbPAL10* (e), and *NbLOX2* (f) in *N. benthamiana* tissues expressing GFP, RipE1, or RipE1 C172A, using Agrobacterium with an OD_{600} of 0.5. Samples were taken at the indicated times after Agrobacterium infiltration. In each case, the RipE1 variants and their respective GFP control were expressed in the same leaf, and values are represented side-by-side. Expression values are relative to the expression of the housekeeping gene *NbEF1a*. Values indicate mean ± SE (n=3). Each experiment was repeated at least 3 times with similar results.

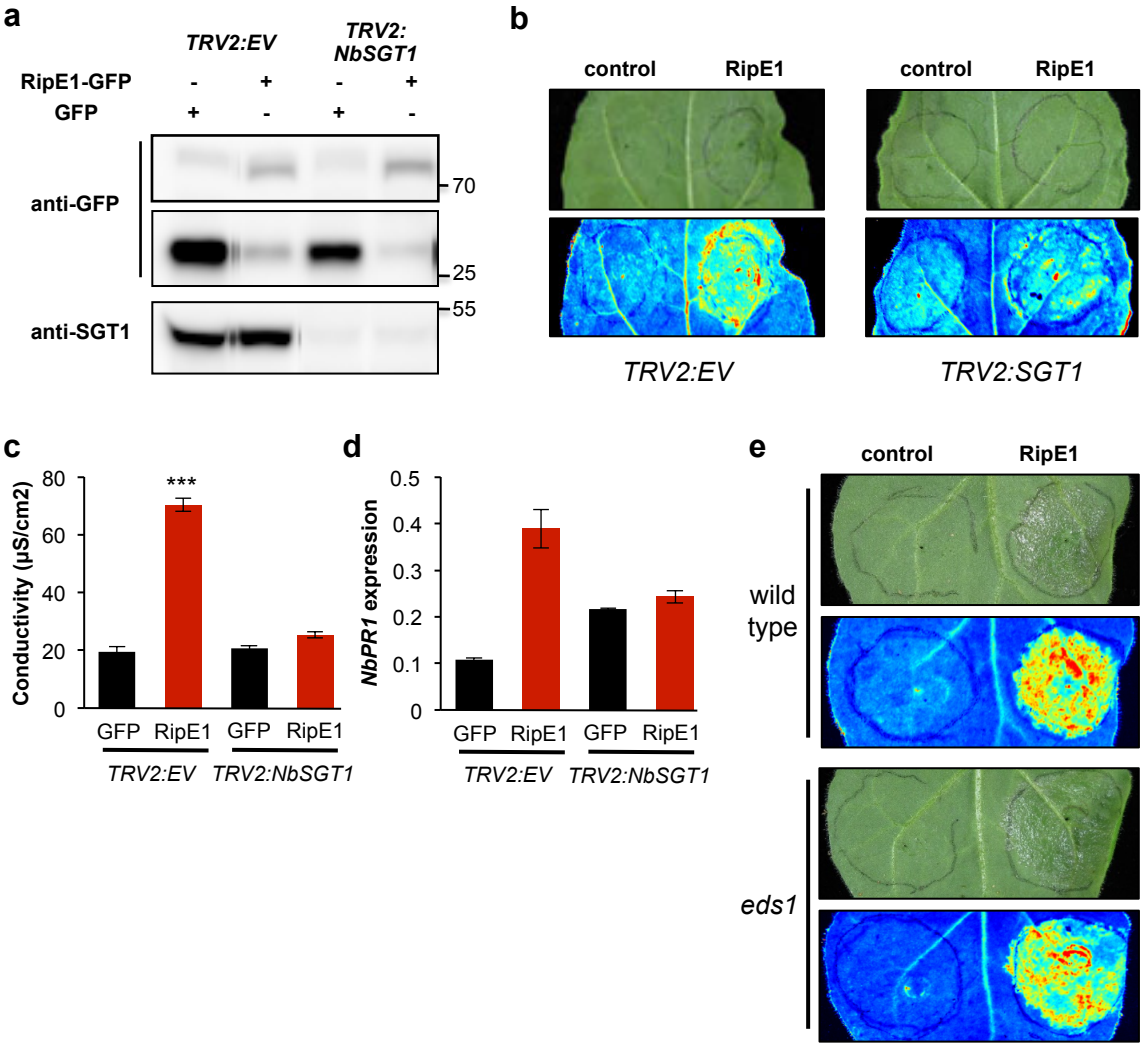

Figure 4. RipE1-triggered responses require SGT1, but not EDS1.
(a-d) RipE1-GFP or GFP (as control) were expressed in the same leaf of *N. benthamiana* undergoing VIGS of *NbSGT1* or VIGS with an empty vector (EV) construct (as control), using Agrobacterium with an OD_{600} of 0.5. (a) Western blot showing the accumulation of GFP, RipE1-GFP, and endogenous *NbSGT1*. Molecular weight (kDa) marker bands are indicated for reference. Vertical lines next to the bands are due to the high sensitivity setting used in the imaging equipment. (b) Photos were taken 2 days post-inoculation with a CCD camera (upper panel) or an UV camera (lower panel). UV signal corresponds to the development of cell death (not GFP fluorescence). UV images were taken from the abaxial side and flipped horizontally for representation. (c) Ion leakage measured in leaf discs taken from *N. benthamiana* tissues expressing RipE1-GFP or GFP (as control), representative of cell death, 48 hours after Agrobacterium infiltration. Values indicate mean ± SE (n=3). (d) Quantitative RT-PCR to determine the expression of *NbPR1* in *N. benthamiana* tissues 48 hours after Agrobacterium infiltration. Expression values are relative to the expression of the housekeeping gene *NbEF1a*. Values indicate mean ± SE (n=3). (e) RipE1-GFP or GFP (as control) were expressed in the same leaf of *N. benthamiana* wild type or a stable *eds1* knockout mutant, using Agrobacterium with an OD_{600} of 0.5. Photos were taken 2 days post-inoculation with a CCD camera (upper panel) or an UV camera (lower panel). UV signal corresponds to the development of cell death (not GFP fluorescence). UV images were taken from the abaxial side and flipped horizontally for representation. Each experiment was repeated at least 3 times with similar results.

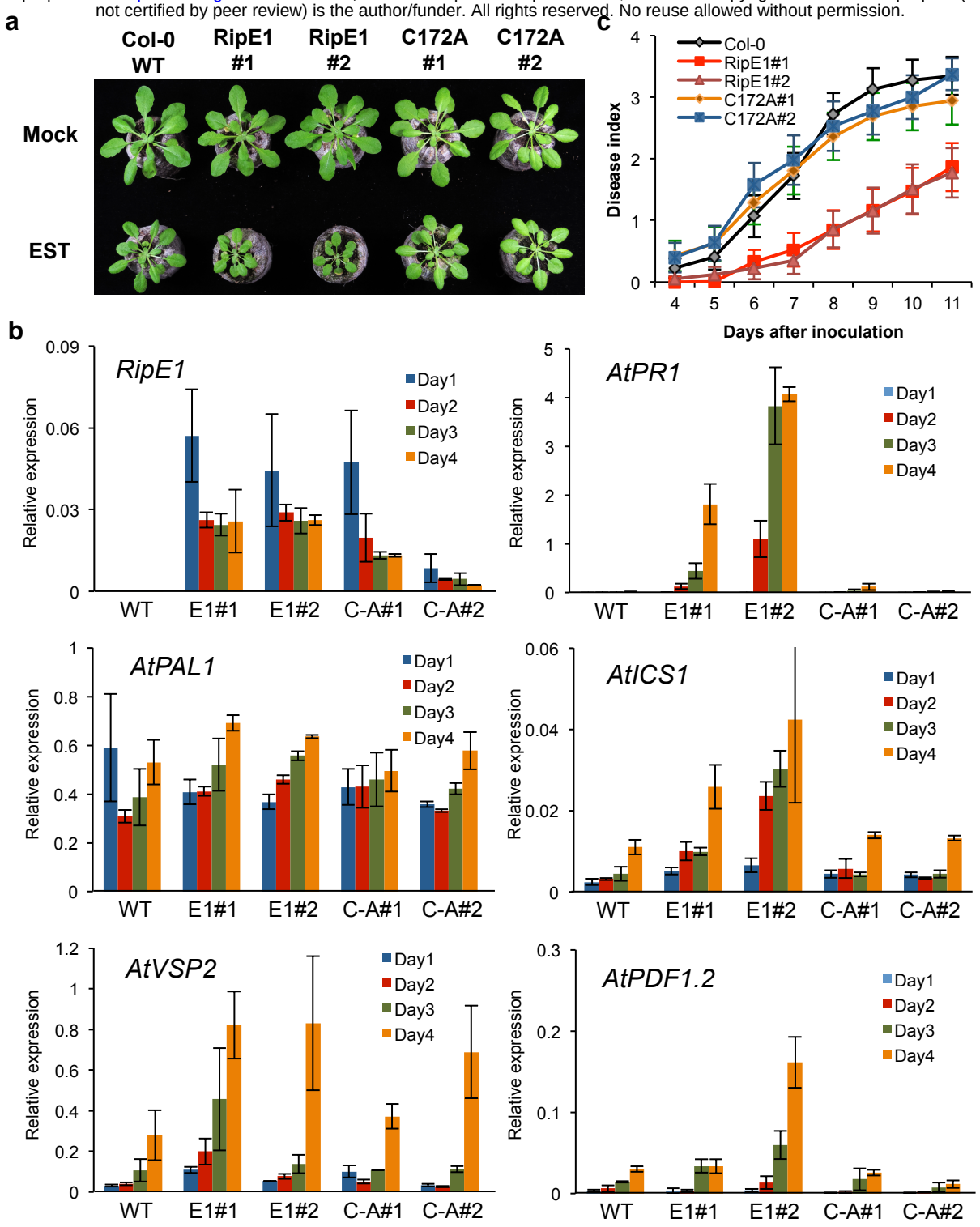

Figure 5. RipE1 triggers immunity in Arabidopsis.
(a) Arabidopsis Col-0 wild type or independent stable transgenic lines expressing RipE1 or RipE1 C172A from an estradiol (EST)-inducible promoter were grown for 3 weeks and then treated sprayed with 100 µM EST daily. Photographs were taken 2 weeks after beginning the EST treatment. (b) Arabidopsis 4 day-old seedlings were treated with 25 µM EST and samples were taken 1, 2, 3, or 4 days after EST treatment. Quantitative RT-PCR to determine the expression of *RipE1, AtPR1, AtPAL1, AtICS1, AtVSP2,* and *AtPDF1.2*. Expression values are relative to the expression of the housekeeping gene *AtACT2*. Values indicate mean ± SE (n=3). (c) Plants in (a) were inoculated with *R. solanacearum* GMI1000 by soil-drenching. The results are represented as disease progression, showing the average wilting symptoms in a scale from 0 to 4 (mean ± SEM). n=20 plants per genotype. Each experiment was repeated at least 3 times with similar results.

Figure 6

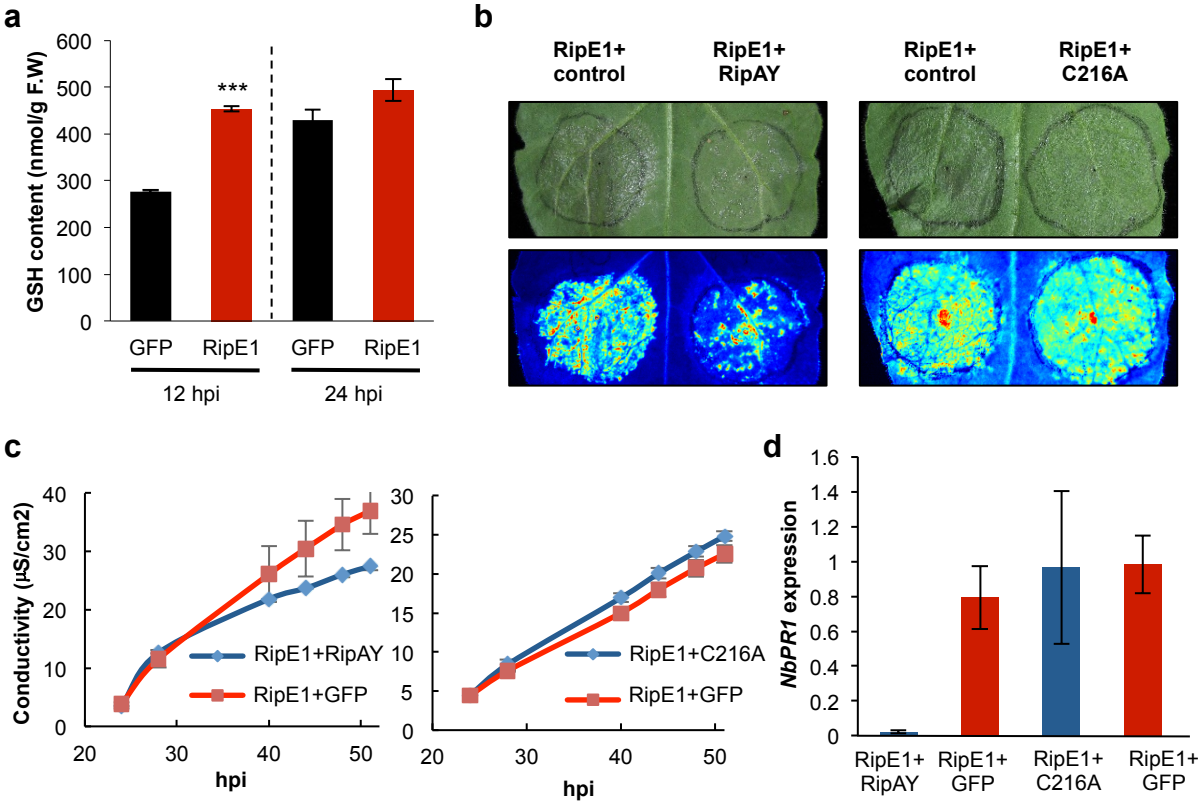

Figure 6. RipE1-triggered immune responses are suppressed by RipAY. (a) RipE1-GFP or GFP (as control) were expressed in the same leaf of *N. benthamiana* using Agrobacterium with an OD_{600} of 0.5, and samples were taken at the indicated time points to measure the accumulation of glutathione (GSH). (b-d) RipE1-Nluc was co-expressed with GFP (as control), with RipAY-GFP, or with RipAY-C216A-GFP, respectively, in the same leaf. Protein accumulation is shown in the figure S6. (b) Photos were taken 2.5 days post-inoculation with a CCD camera (upper panel) or an UV camera (lower panel). UV signal corresponds to the development of cell death (not GFP fluorescence). UV images were taken from the abaxial side and flipped horizontally for representation. (c) Ion leakage measured in leaf discs taken from *N. benthamiana* tissues expressing RipE1 together with GFP or NahG-GFP, representative of cell death, at the indicated timepoints. Values indicate mean ± SE (n=3). (c) Quantitative RT-PCR to determine the expression of *NbPR1* in *N. benthamiana* tissues 48 hours after Agrobacterium infiltration. Expression values are relative to the expression of the housekeeping gene *NbEF1a*. Values indicate mean ± SE (n=3). Each experiment was repeated at least 3 times with similar results.

Figure S1

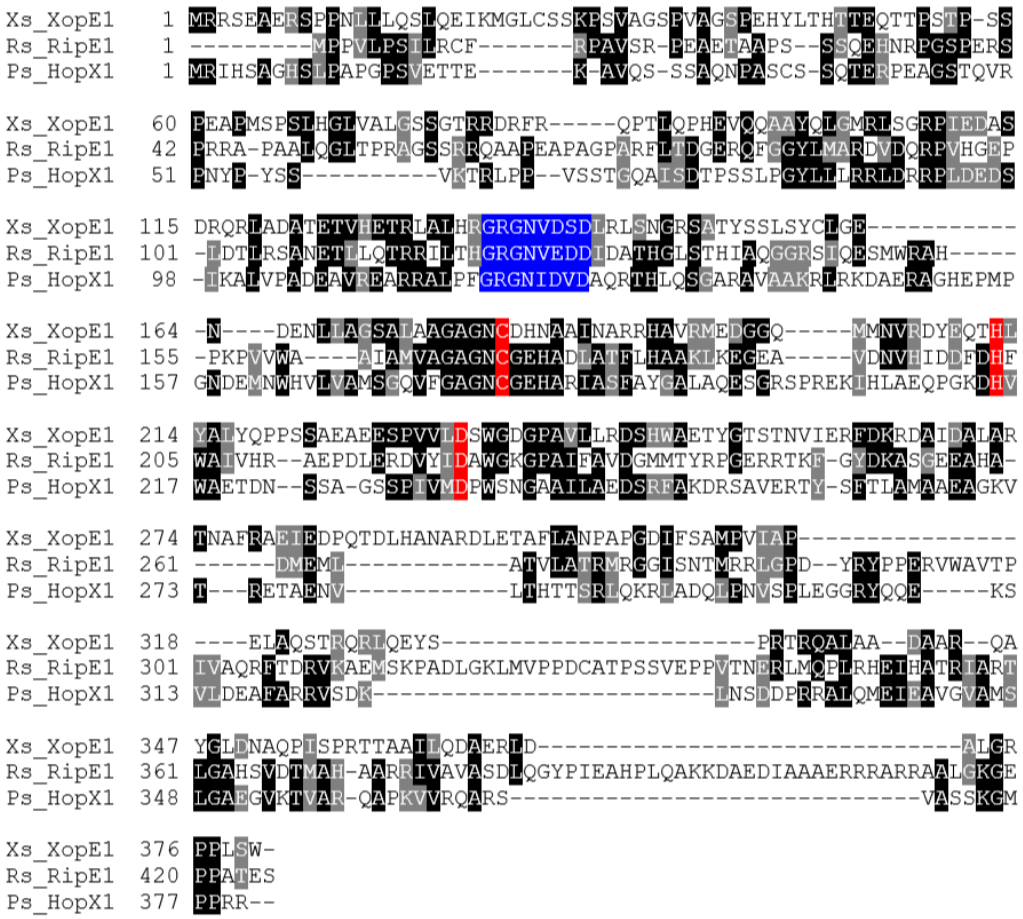

Figure S1. Phylogenetic analysis of RipE1

Alignment of the amino acid sequence of RipE1 from *R. solanacearum* GMI1000 (Rs_RipE1), XopE1 from *Xanthomonas campestris* pv. *vesicatoria* (Xs_XopE1), and HopX1 from *Pseudomonas syringae* pv tabaci 11528 (Ps_HopX1). Residues forming the predicted catalytic triad are indicated in red, and the conserved domain A is indicated in blue. The black shaded amino acids are identical among the three effectors.

Figure S2

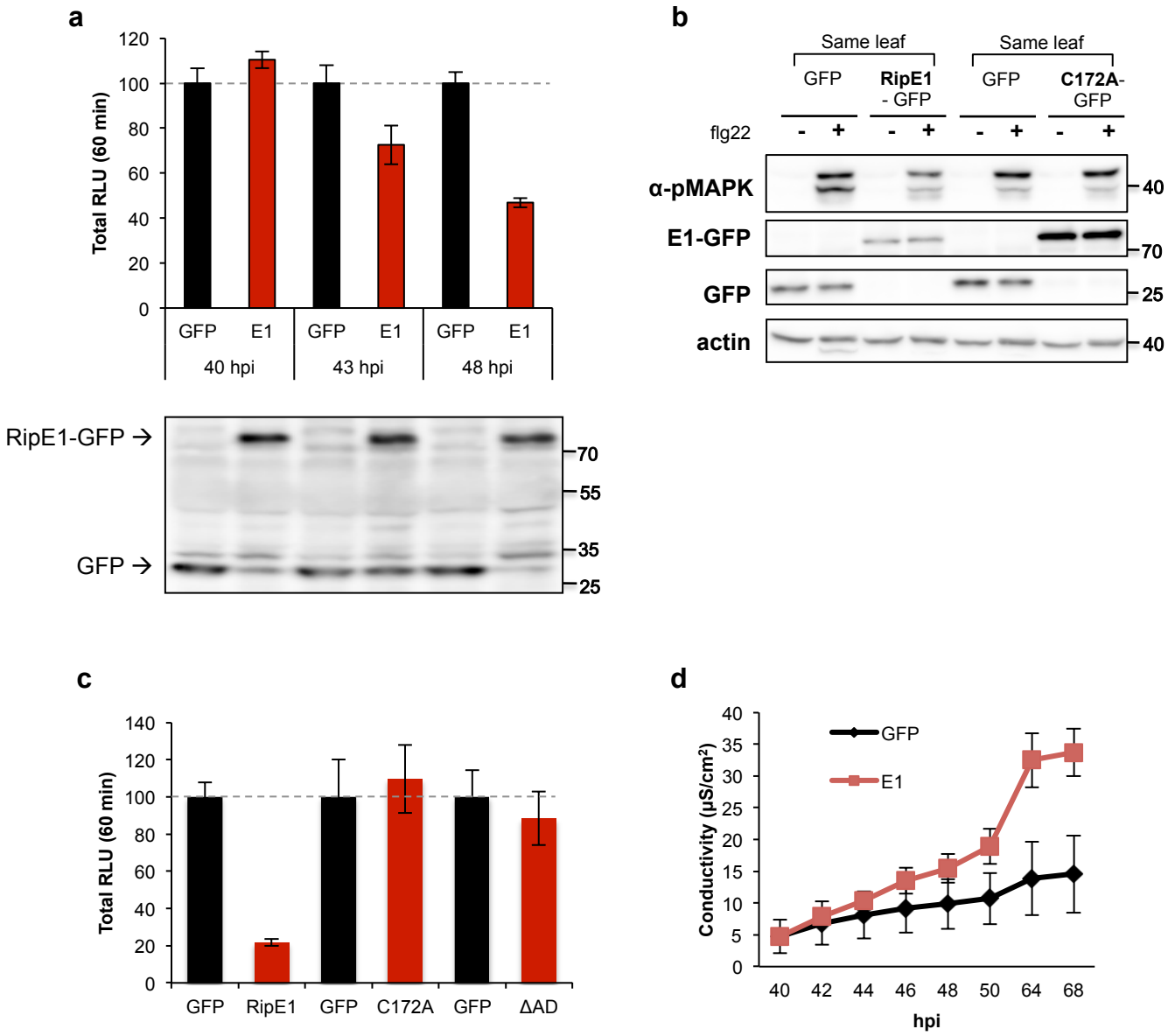

Figure S2. RipE1 expression inhibits PTI responses in *N. benthamiana*, which correlates with the induction of cell death.
Agrobacterium was used to induce the transient expression of RipE1-GFP in half of the leaf and GFP in the other half. (a) Oxidative burst triggered by 50 nM flg22 in *N. benthamiana* tissues at the indicated time points, measured in a luminol-based assay as relative luminescence units (RLU). Values are average ± SE (n=24), and are represented as % of the GFP control in each time point. Western blot with anti-GFP is shown for reference of protein accumulation at each time point. (b) MAPK activation was induced 40 hours after Agrobacterium infiltration with 100 nM flg22 and analysed 15 minutes after flg22 treatment using anti-phosphorylated MAPK antibody (anti-pMAPK). Immunoblots were also analysed using anti-GFP antibody to verify protein accumulation. Anti-actin was used to verify equal loading. Molecular weight (kDa) marker bands are indicated for reference. (c) Oxidative burst was induced as in (a) and measured 2 days post-Agrobacterium infiltration. Mutant variants are described in the Figure 1. (d) Ion leakage was measured as in the Figure 1. Measurement over time after RipE1 expression reflects that the induction of cell death correlates in time with the suppression of PTI responses. The experiments were repeated three times with similar results.

Figure S3

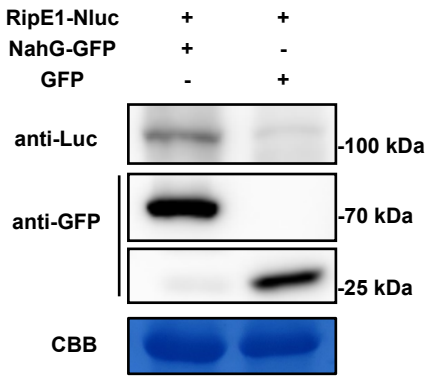

Figure S3. Protein accumulation upon co-expression of RipE1 and NahG.
Western blot showing protein accumulation in the experiments shown in the figure 2. Molecular weight (kDa) marker bands are indicated for reference.

Figure S4

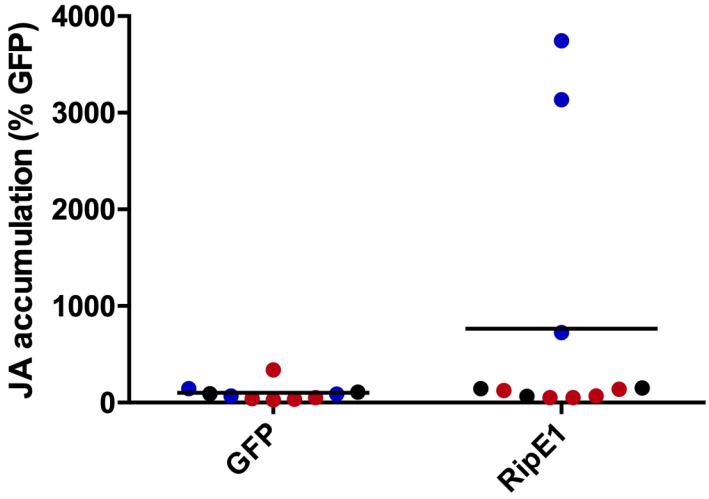

Figure S4. RipE1 expression leads to an increase in JA contents.
Measurement of JA accumulation in *N. benthamiana* tissues expressing GFP or RipE1, using Agrobacterium with an OD_{600} of 0.5. Samples were taken 42 hours after Agrobacterium infiltration. Three independent biological repeats were performed, and the different colors indicate values from different replicates. Values are represented as % of the GFP control in each replicate.

Figure S5

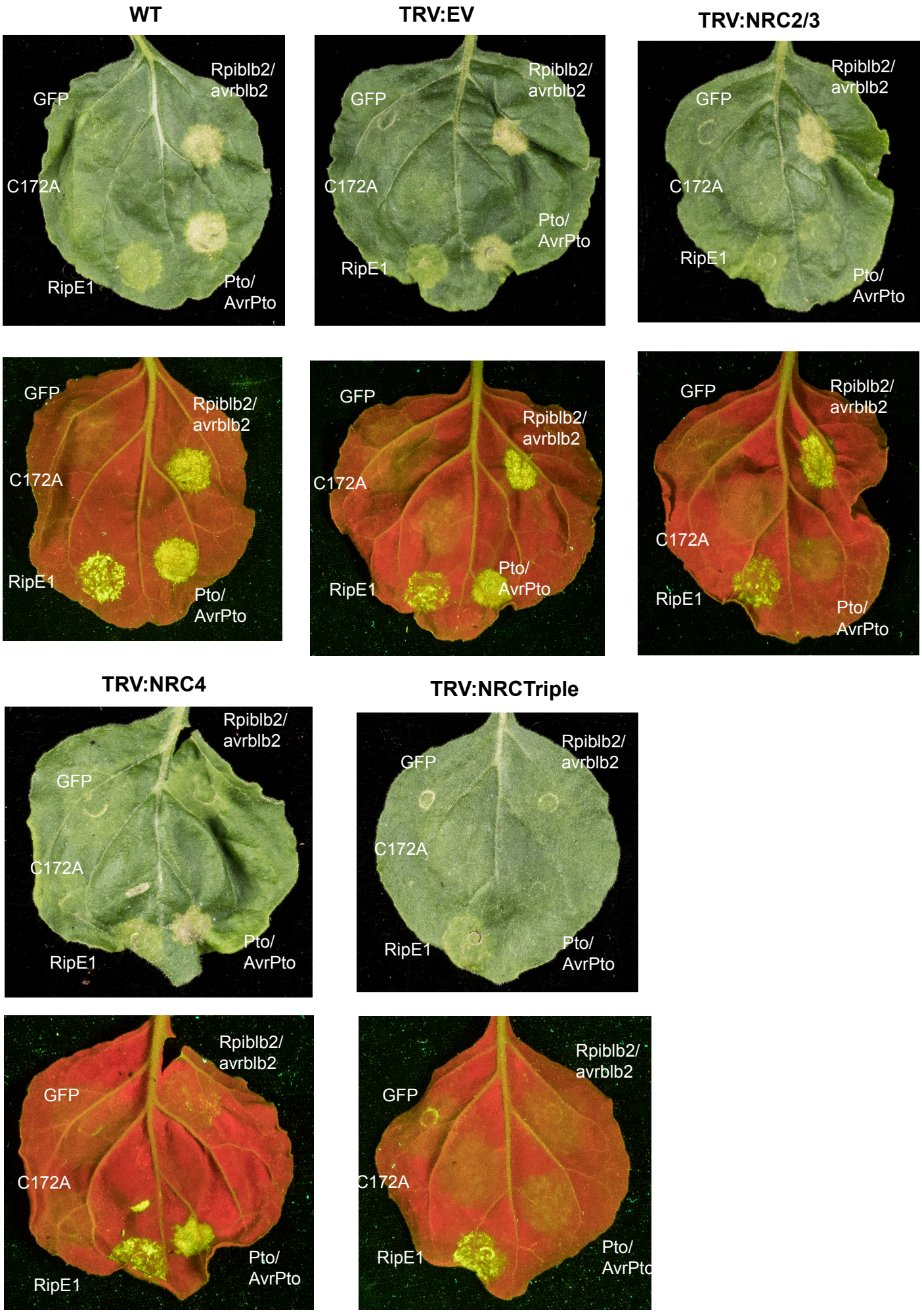
WT
TRV:EV
TRV:NRC2/3
GFP
Rpiblb2/
avrblb2
C172A
RipE1
Pto/
AvrPto
TRV:NRC4
TRV:NRCTriple

Figure S5. RipE1-triggered cell death does not require NRC proteins.
RipE1-GFP, C172A or GFP (as control) were transiently expressed using agrobacterium into wild type (WT) *N. benthamiana*, leaves silenced with EV (as control) and those silenced with different NRC homologs (NRC2/3, NRC4 and NRC2/3/4-Triple), using VIGS. For RipE1-GFP, C172A and GFP an OD_{600} of 0.5 was used. Rpiblb2 (OD_{600} 0.2)/AVRblb2 (OD_{600} 0.1) and Pto (OD_{600} 0.6)/AVRPto (OD_{600} 0.1), which are NRC4 and NRC2/3 dependent, respectively, were included as controls. Photos were taken 5 days post inoculation under natural or UV light. UV images were taken from the abaxial side and flipped horizontally for representation.

Figure S6

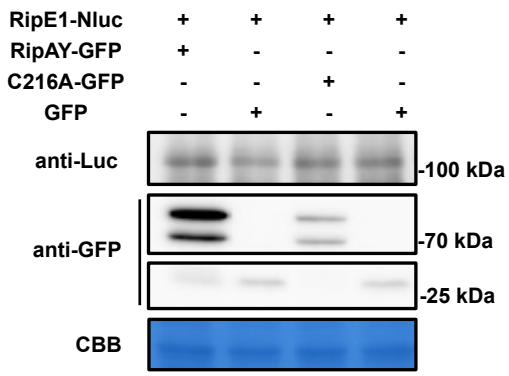

Figure S6. Protein accumulation upon co-expression of RipE1 and RipAY.
Western blot showing protein accumulation in the experiments shown in the figure 6. Molecular weight (kDa) marker bands are indicated for reference.